Electronic transport as a tool to study the microscopic structure of a density-wave state

Pavel Grigoriev

L. D. Landau Institute for Theoretical Physics,
Chernogolovka, Russia

Russian Academy of Sciences
L. D. Landau
Institute for
Theoretical
Physics

What information about DW can be obtained from simple electronic transport measurements?

Puzzling experimental data and their explanation will be presented

Part 1: temperature dependence of conductivity anisotropy

Part 2: huge maximum of longitudinal interlayer magnetoresistance and the phase inversion of magnetic quantum oscillations (SdH)

Why magnetoresistance studies are important?

There are only few methods to study electronic dispersion $E(p)$ and Fermi surface (FS) geometry in metals, including strongly-correlated systems with competing orders.

These methods include:

1. **Conductivity tensor $\sigma_{ij} \propto e^2 \tau \langle v_i v_j \rangle_{FS} = \sigma_{ij}(T)$ gives only general information about anisotropy of $E(p)$ and about phase transitions with lowering temperature.**
2. **Band-structure calculations** (rough, not always reliable)
3. **ARPES (Angle resolved photoemission spectroscopy)** **Drawbacks: (i) Not always available; (ii) Only surface electrons participate; (iii) low resolution >10meV.**
4. **Magnetotransport: angular and field dependence of MR, including magnetic quantum oscillations (powerful tool, useful both alone or as complementary to ARPES).**

ARPES (Angle resolved photoemission spectroscopy)

Main idea:

$$E = \hbar\omega - E_k - \phi$$

E_k = kinetic energy of the outgoing electron — can be measured.
$\hbar\omega =$ incoming photon energy - known from experiment, φ = known electron work function.
Angle resolution of photoemitted electrons gives their momentum.

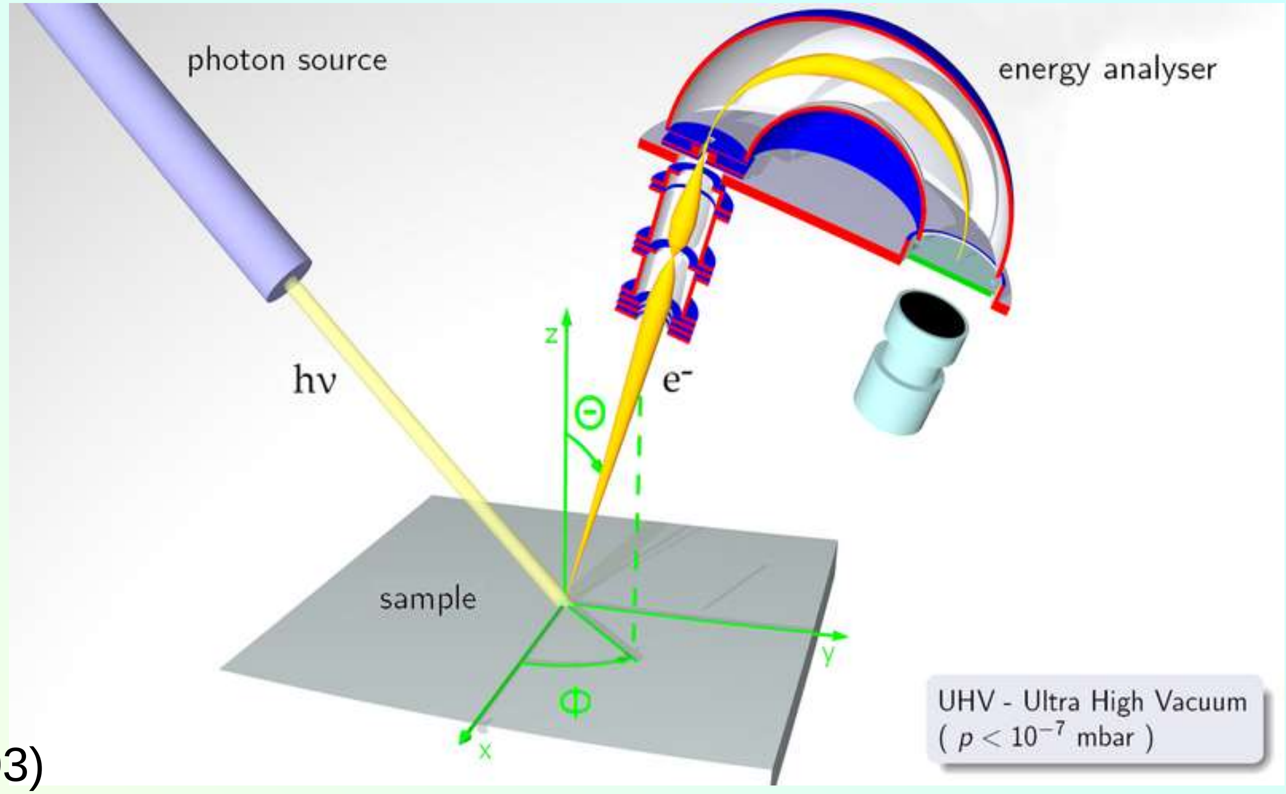

Rev.Mod.Phys. 75, 473 (2003)

The photocurrent intensity is proportional to a one-particle spectral function multiplied by the Fermi function:

$$I(\mathbf{k},\omega) = A(\mathbf{k},\omega)f(\omega)$$

$$A(\omega,\mathbf{k}) = -\frac{1}{\pi}\frac{\Sigma''(\omega)}{(\omega-\varepsilon(\mathbf{k})-\Sigma'(\omega))^2+\Sigma''(\omega)^2}.$$

Therefore can find out information about *E(k)*

Drawbacks: 1) Often unavailable; 2) Only surface electrons participate.

ARPES data and Fermi-surface shape

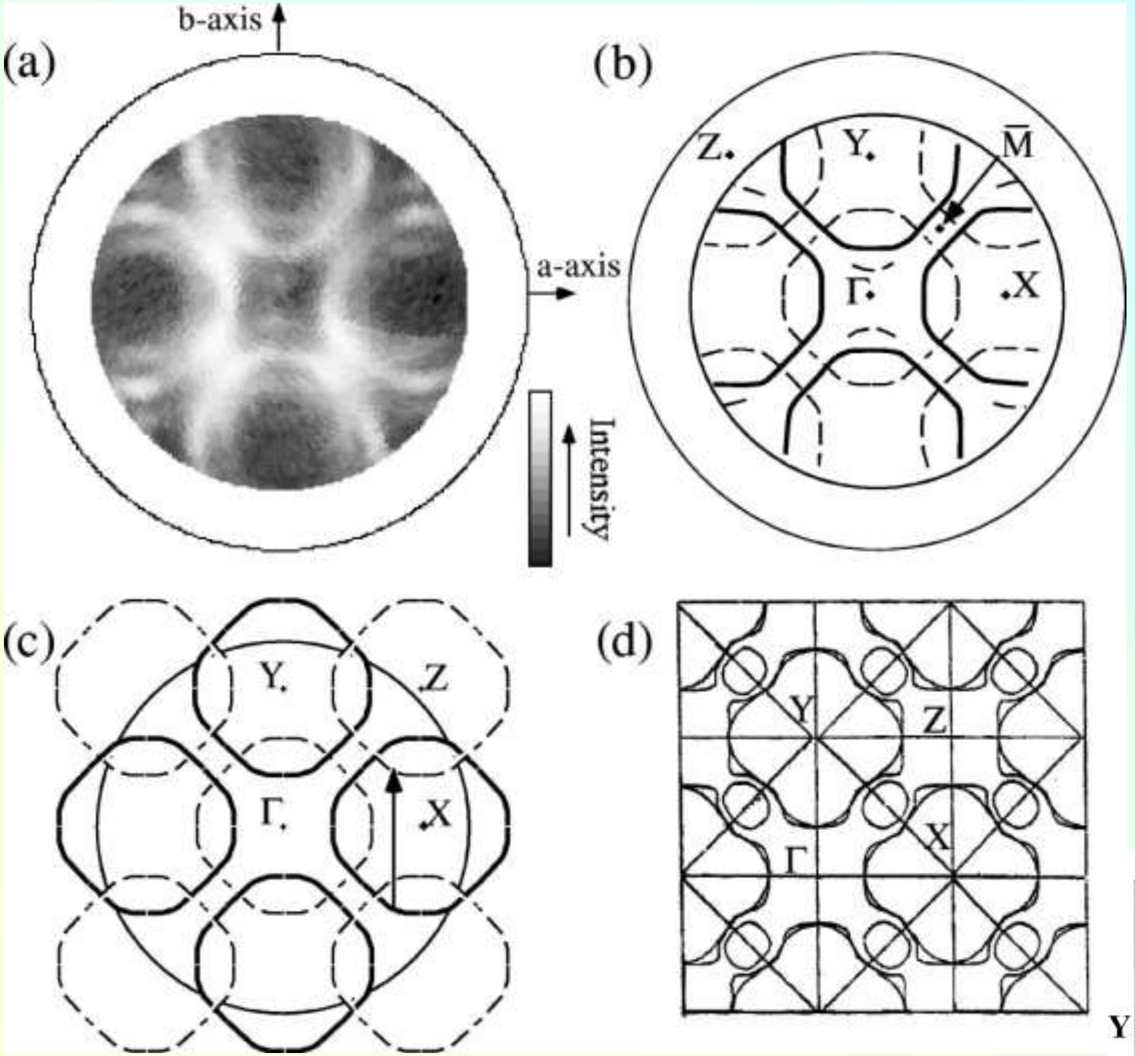

The Fermi surface of near optimally doped $Bi_2Sr_2CaCu_2O_{8+\delta}$ (a) integrated intensity map (10-meV window centered at *EF*) for Bi2212 at 300 K obtained with 21.2-eV photons (HeI line); (b),(c) superposition of the main Fermi surface (thick lines) and of its (p,p) translation (thin dashed lines) due to backfolded shadow bands; (d) Fermi surface calculated by Massidda *et al.* (1988).

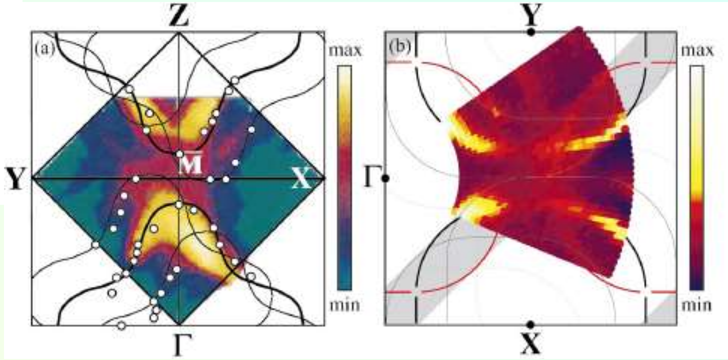

Drawback 3: Low resolution
=> ambiguous interpretation

Phase diagram of high-Tc cuprate SC. Importance of magnetoresistance studies.

$Nd_{2-x}Ce_xCuO_4$ (NCCO)

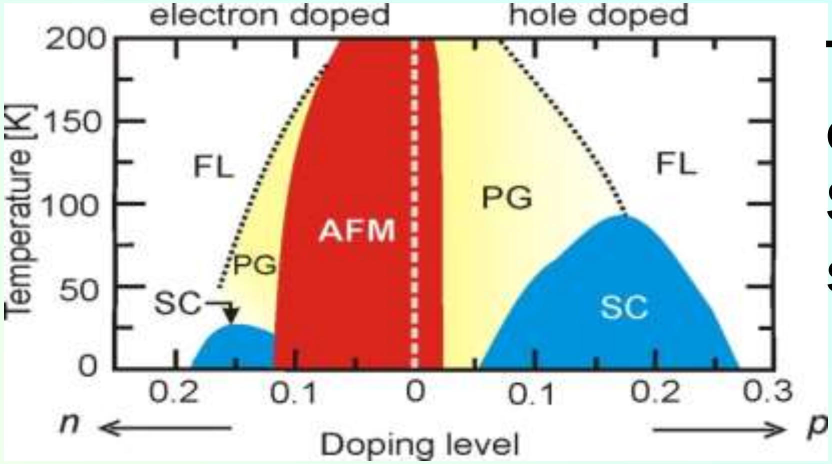

Theory predicts shift of the QPT point in SC phase? How strong is this shift?

Original FS:

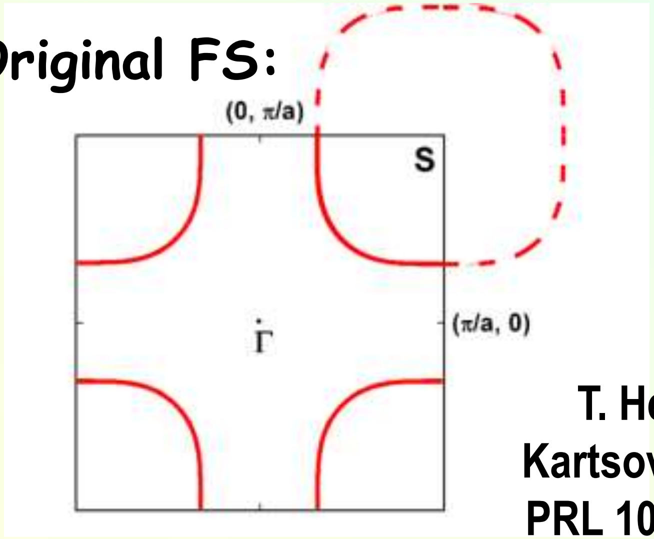

<u>n = 0.17</u>

S_h = 41.5% of S_{BZ}

T. Helm, M. Kartsovnik et al., PRL 103, 157002 (2009)

Reconstructed FS:

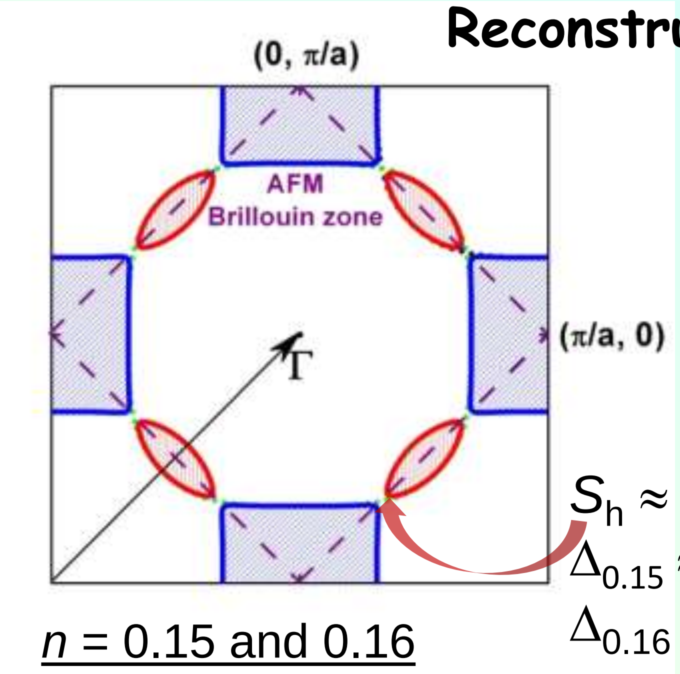

<u>n = 0.15 and 0.16</u>

$S_h \approx 1.1\%$ of S_{BZ};
$\Delta_{0.15} \approx 64$ meV;
$\Delta_{0.16} \approx 36$ meV

Peierls instability and density wave

If the electron dispersion satisfies nesting condition:

$$\boxed{\varepsilon(k)+\varepsilon(k+Q_N)=0}$$

(at least on some finite part of the Fermi surface in metals),

the susceptibility $\chi(Q_N)$ diverges. Then at low temperature any e-e interaction leads to a new many-body state, which is a charge- or spin-density wave (CDW or SDW).

Main features of CDW/SDW:

A gap in electron spectrum appears in CDW or SDW state. If this gap covers the whole FS, the metal becomes an insulator.

The modulation of charge or spin electron density can be detected by x-ray for CDW and by NMR, neutron or muon scattering for SDW.

Geometrical interpretation of nesting condition

Quasi-1D metals

$$\boxed{\varepsilon(k) = v_F(|k| - k_F) - 2t_y\cos(k_y b)}$$

satisfies nesting condition:

$$\boxed{\varepsilon(k) + \varepsilon(k + Q_N) = 0}$$

with $\boxed{Q_N = (2k_F, \pi / b).}$

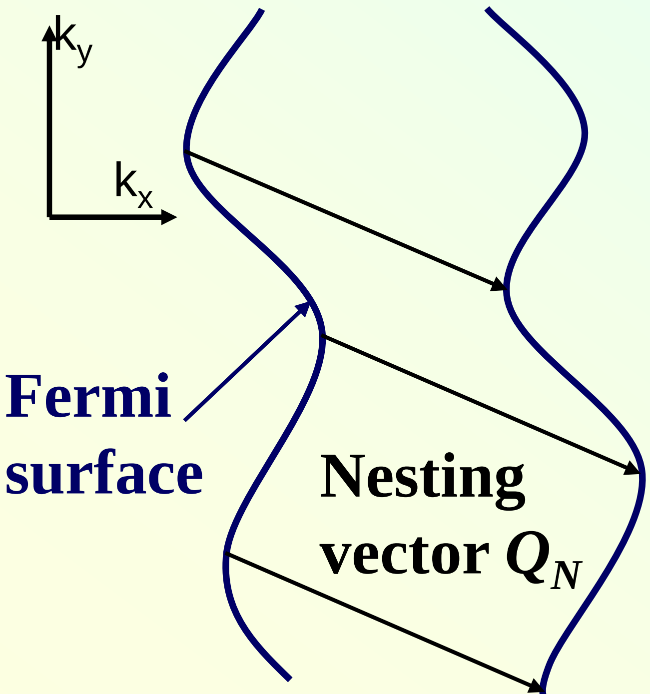

Quasi-2D metals

hidden1D anisotropy

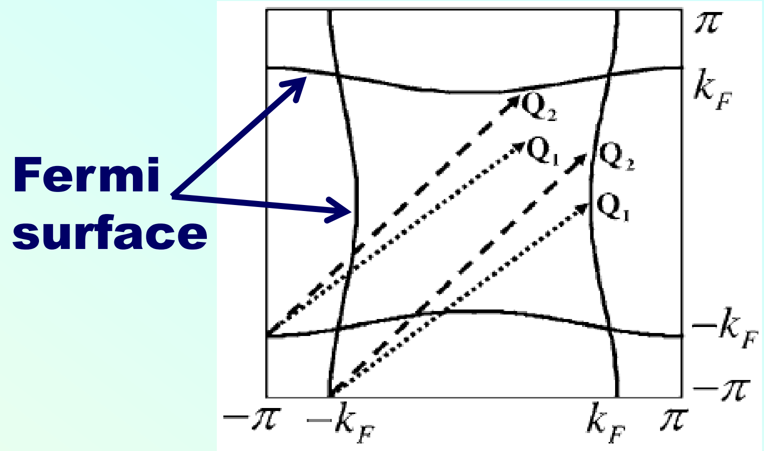

3D metals

partial nesting

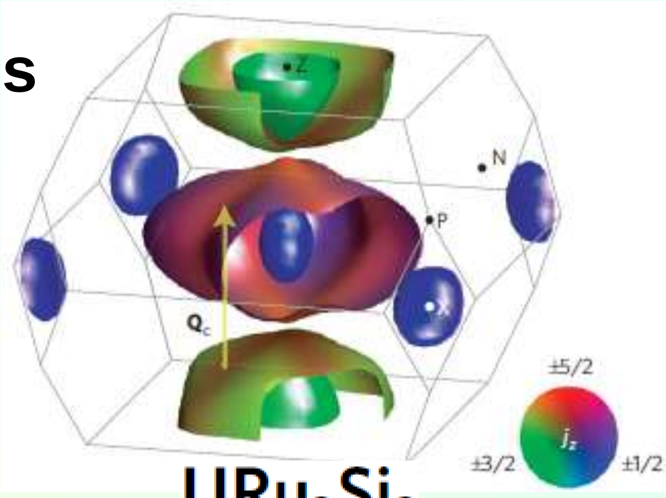

URu_2Si_2

Peierls transition in 1D metals

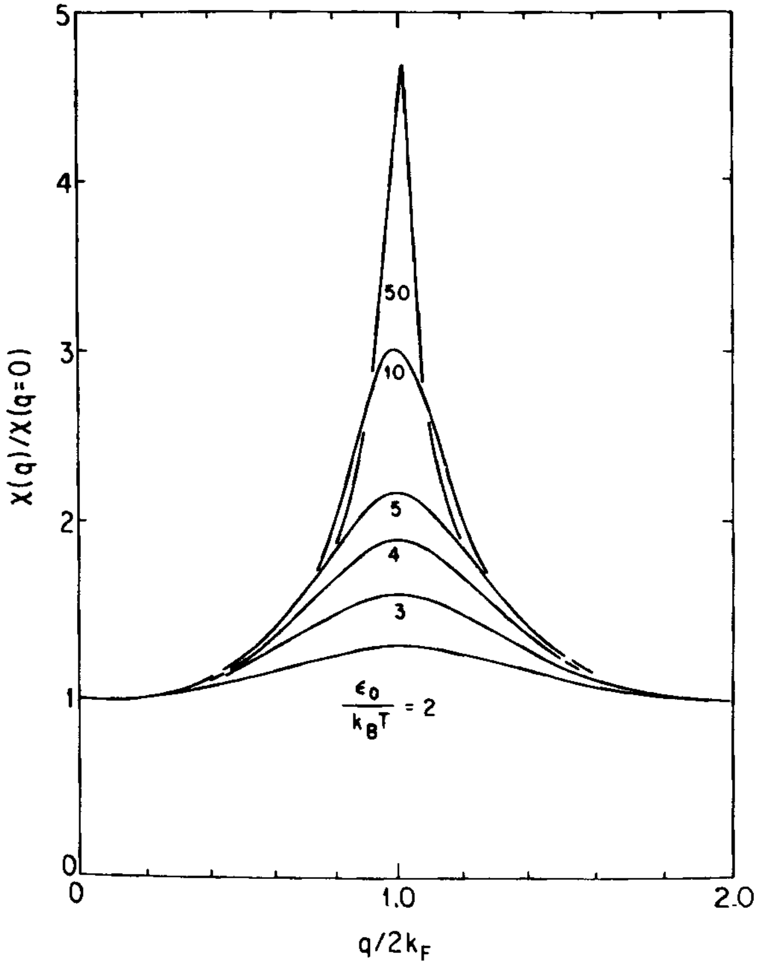

Electronic susceptibility as function wave vector and temperature

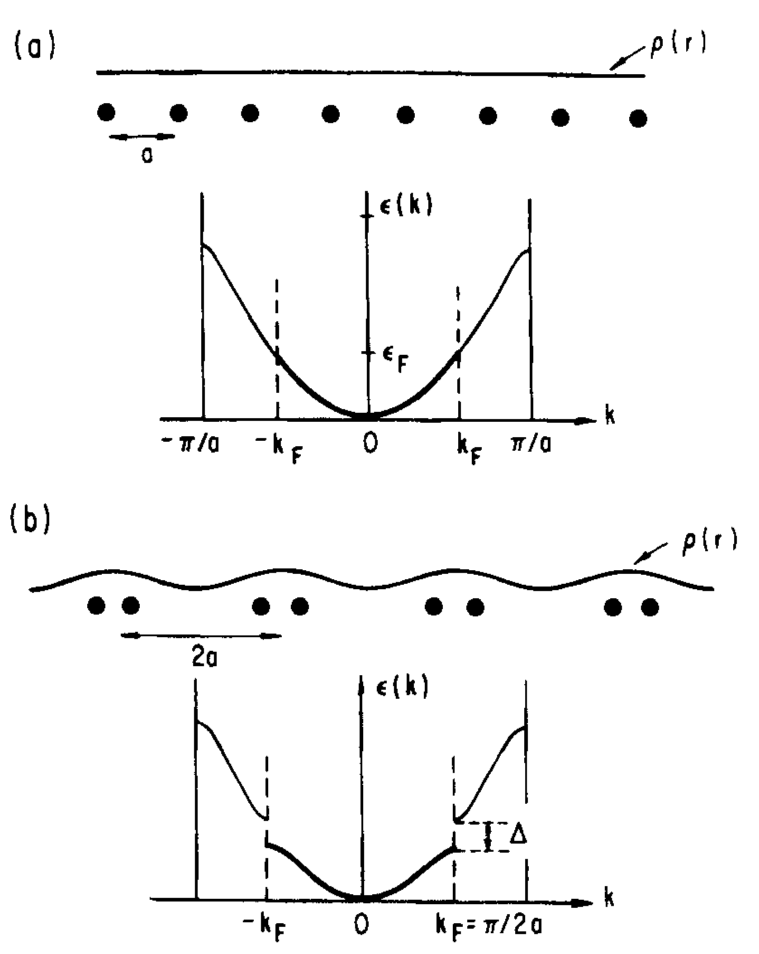

Electron density and lattice distortion for half-filled band

G. Gruener, *Density waves in Solids*, 1994

Charge- and spin-density wave

Charge-density wave

Density modulations for two spin components in CDW:

$$\rho_\uparrow(x) = \rho_0 + \Delta\cos(Qx) = \rho_\downarrow(x)$$

$$\rho_\uparrow(x) = \rho_\downarrow(x)$$

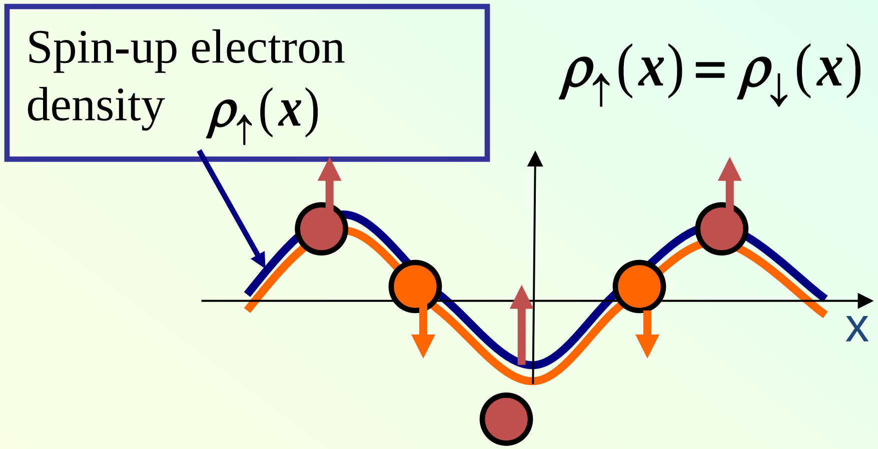

Total charge density is modulated

$$\rho_C(x) = \rho_\uparrow(x) + \rho_\downarrow(x) = 2\left[\rho_0 + \Delta_0 \cos\left(Q\,x\right)\right]$$

Total spin density is constant

$$\rho_S(x) = \rho_\uparrow(x) - \rho_\downarrow(x) = 0.$$

Spin-density wave

Density modulations for two spin components in SDW:

$$\boldsymbol{\rho_\uparrow(x) = \rho_0 + \Delta\cos(Qx)}$$

$$\boldsymbol{\rho_\downarrow(x) = \rho_0 - \Delta\cos(Qx)}$$

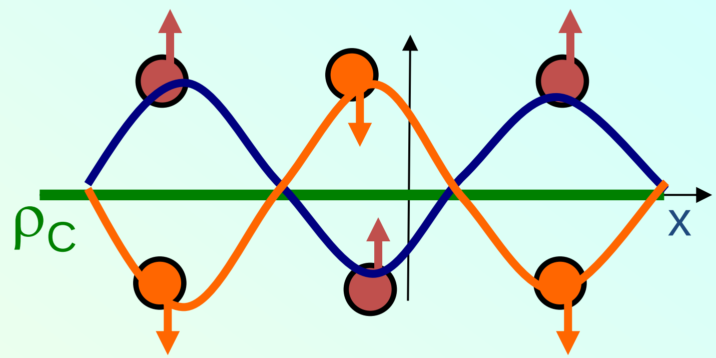

Total charge density is constant:

$$\rho_C(x) = \rho_\uparrow(x) + \rho_\downarrow(x) = const\,:$$

Total spin density has modulation

$$\rho_S(x) = \rho_\uparrow(x) - \rho_\downarrow(x) = 2\Delta_0 \cos\left(Q\,x\right).$$

STM images of CDW

STM images of the (*b, c) plane of NbSe3, scanned area 20 × 20 nm2.*
(a)T = 77 K. Vbias = +100 mV, I = 1 nA.
(b) Fourier transform of the STM image.
(c) *T = 5K, Vbias = +200mV, I = 150 pA*
The Q2 CDW appears
(d) 2D Fourier transform of the STM image shown in (c).

CDW transition temperatures :
T_{P1}= 144K and T_{P2}= 59K

CDW can be visually observed via STM as intensity modulation.

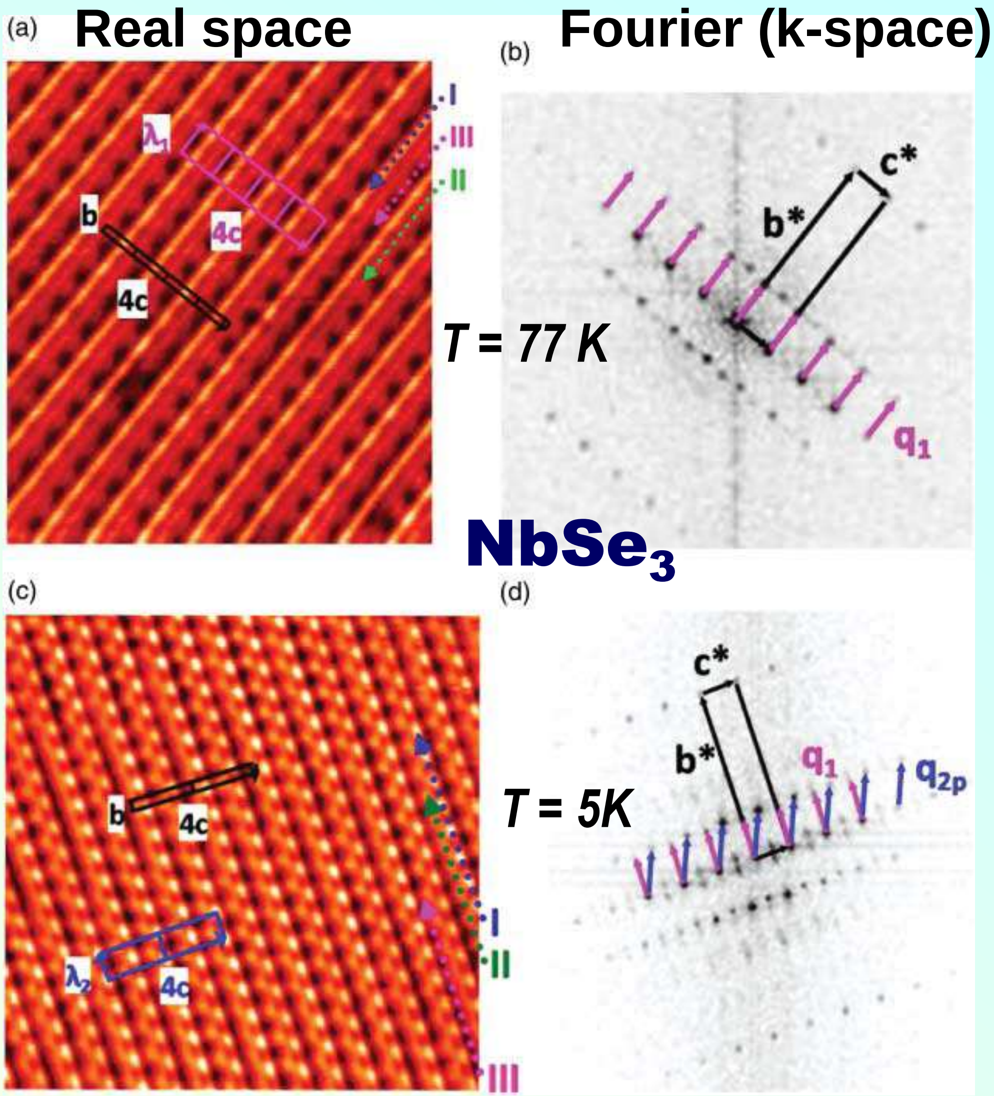

C. Brun *et al.*, PRB 80, 045423 (2009)

also in P. Monceau, Adv. Phys. 61, 325 (2012)

CDW / SDW band structure

Electron Hamiltonian in the mean field approximation:

$$\hat{H}_Q = \sum_{k\sigma} \varepsilon_\sigma(k) a_\sigma^+(k) a_\sigma(k) + \sum_{k\sigma} \hat{\Delta}_Q a_\sigma^+(k+Q) a_\sigma(k).$$

The order parameter $\hat{\Delta} \equiv g \sum_{k'\sigma'} a_{\sigma'}^+(k'-Q) a_{\sigma'}(k')$

is a number for CDW, and a spin operator for SDW: $\hat{\Delta}_Q = \Delta_0(\hat{\sigma} \cdot l).$

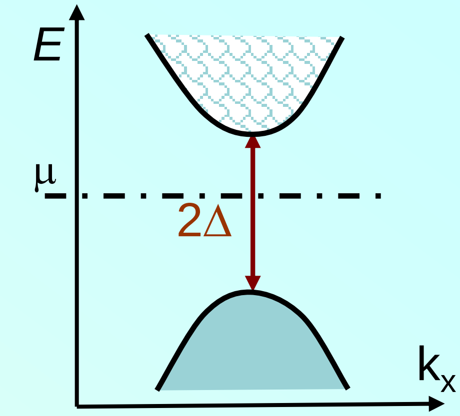

Energy band diagrams

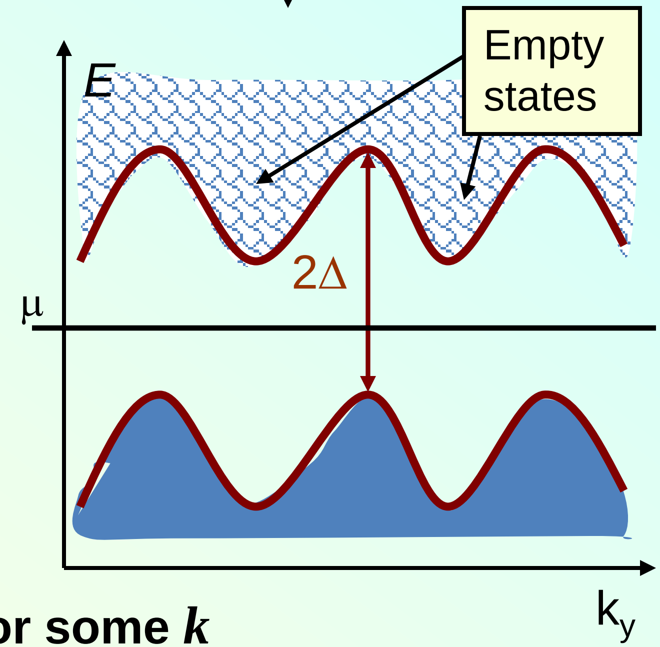

Energy spectrum in the CDW /SDW state

$$E(k) = \frac{\varepsilon(k) + \varepsilon(k+Q_N)}{2} + \sqrt{\left(\frac{\varepsilon(k) - \varepsilon(k+Q_N)}{2}\right)^2 + \Delta^2}.$$

Perfect nesting condition: $\varepsilon(k) + \varepsilon(k+Q_N) = 0.$

Partial nesting condition: $\varepsilon(k) + \varepsilon(k+Q_N) > \Delta$ **for some *k***

Typical resistivity behavior during the CDW/SDW phase transition

1. Total FS is gapped => exponential (insulating) temperature dependence

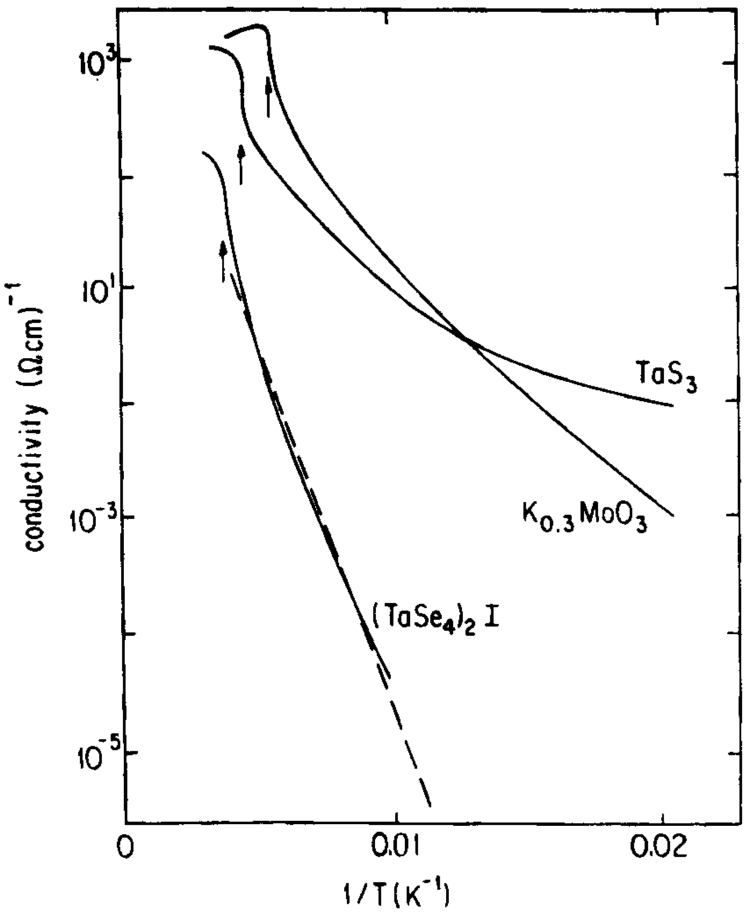

2. FS is partially gapped => temperature dependence of R is metallic with jump at T_p and different slope in a CDW state.

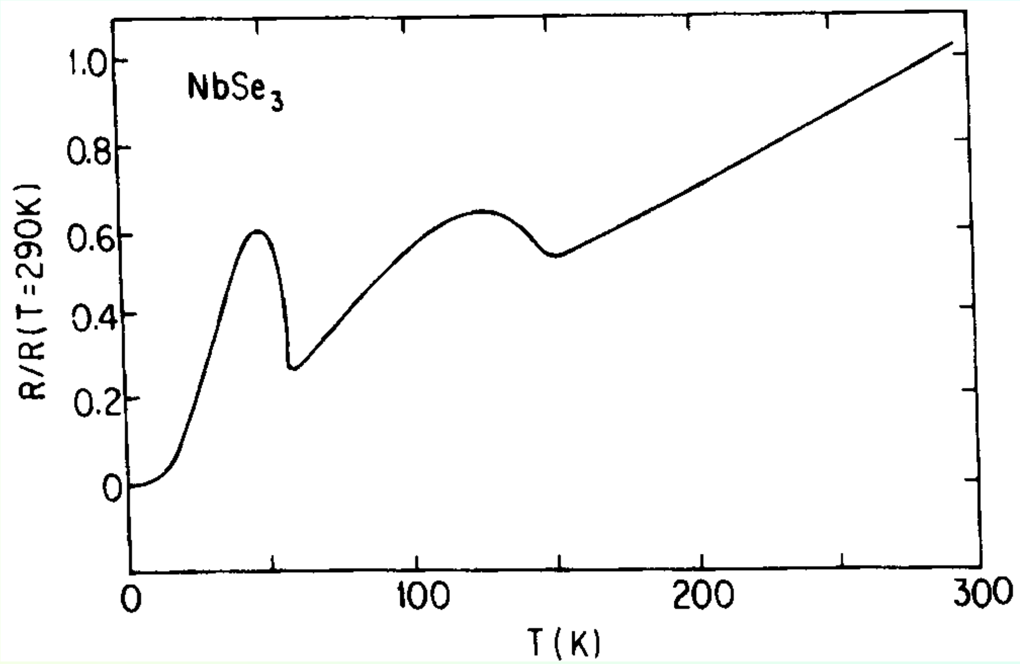

G. Gruener, *Density waves in Solids*, 1994

Part 1

Spontaneous breaking of isotropy observed in the electronic transport of rare-earth tritellurides

or

In-plane conductivity anisotropy caused by the charge density wave state in rare-earth tritellurides

and how it can be used to reveal the microscopic structure of the DW state

A.A. Sinchenko, P.D. Grigoriev, P. Lejay, P. Monceau, Phys. Rev. Lett. 112, 036601 (2014)

Experimental data:

Anisotropy of in-plane conductivity in RTe_3

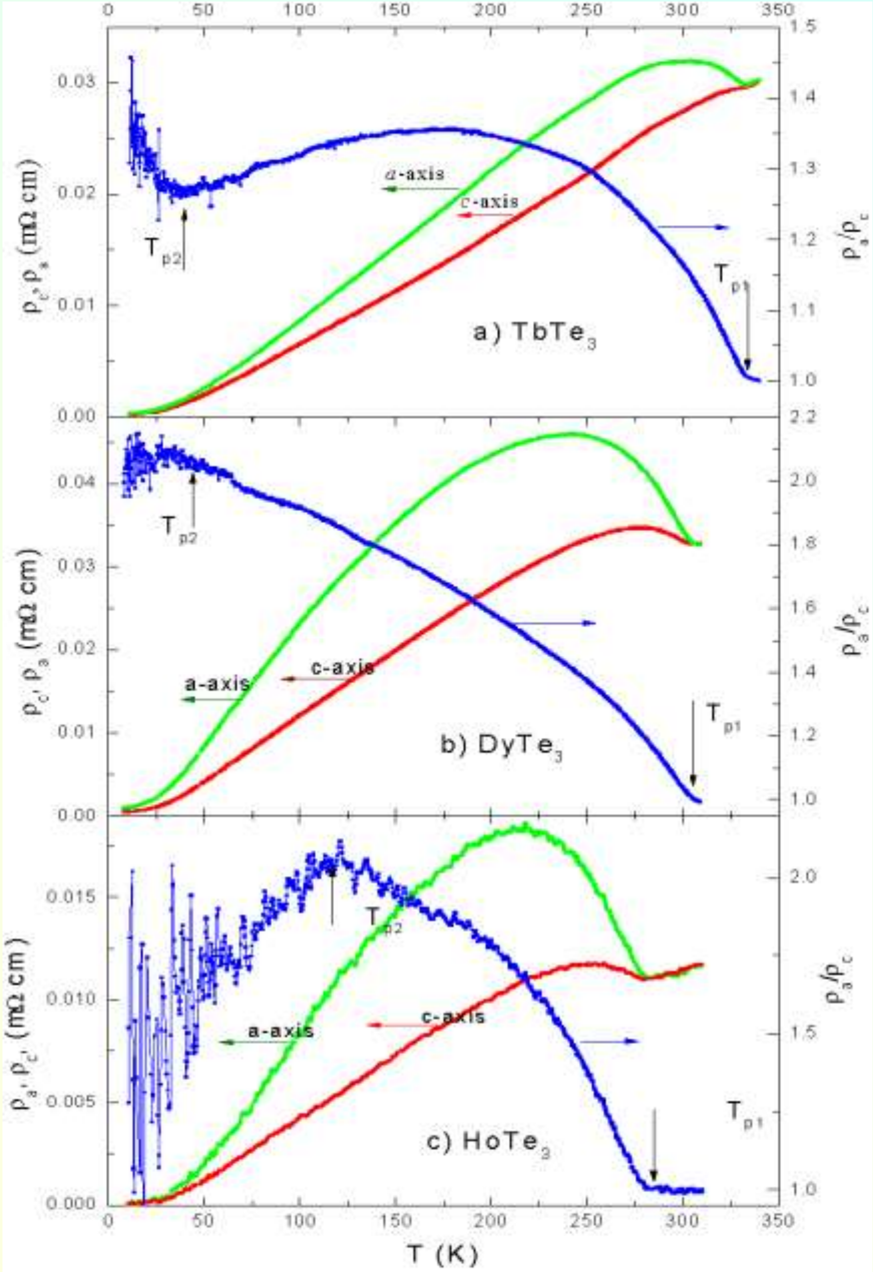

Experimental observations:

Above CDW transition temperature T_{p1} (=336K for $TbTe_3$) the in-plane conductivity is isotropic: $\rho_c = \rho_a$

Below T_{p1} the in-plane conductivity is anisotropic: $\rho_a > \rho_c$

Resistivity increases stronger in the direction $a \perp Q_N \parallel c$, which expels domain-wall CDW scenario

Notations:

a and c along conducting layers

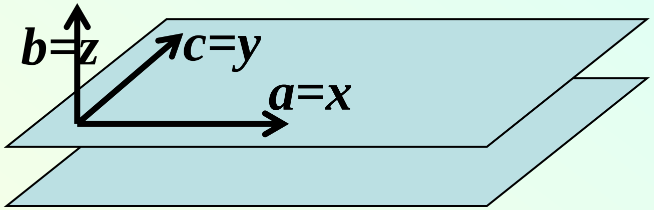

Crystal structure of rare-earth tritellurides RTe_3

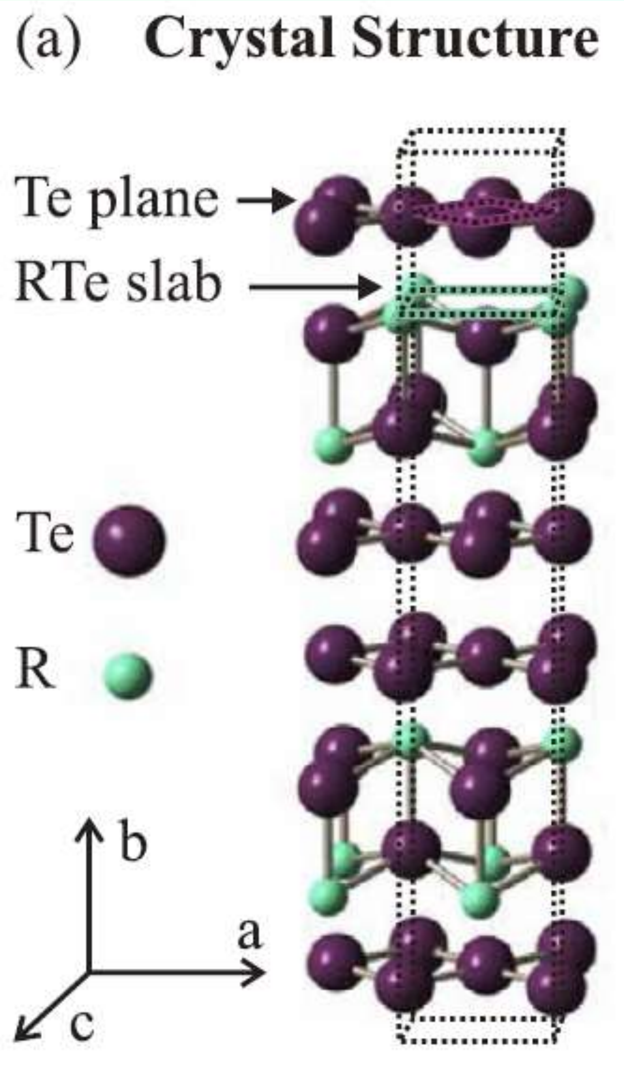

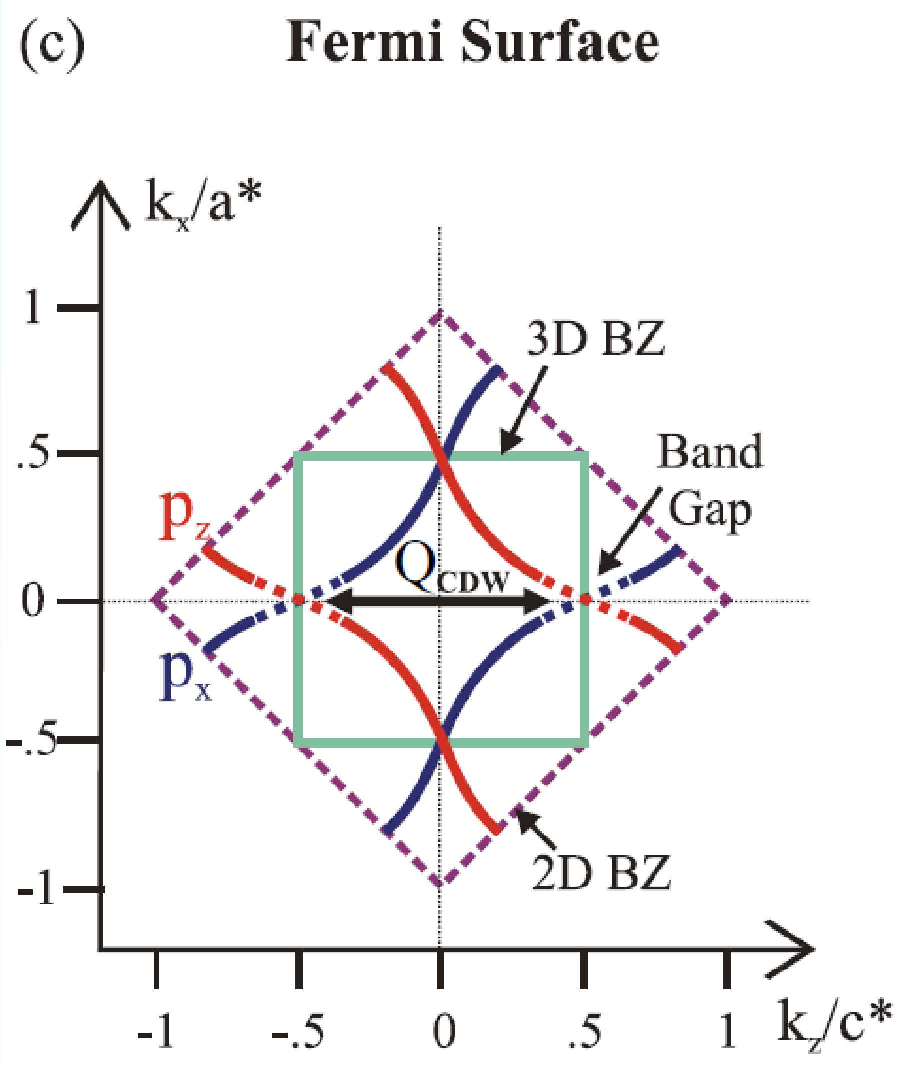

F. Schmitt et al., New Journal of Physics 13, 063022 (2011)

ARPES data on momentum dependence of CDW energy gap in $TbTe_3$

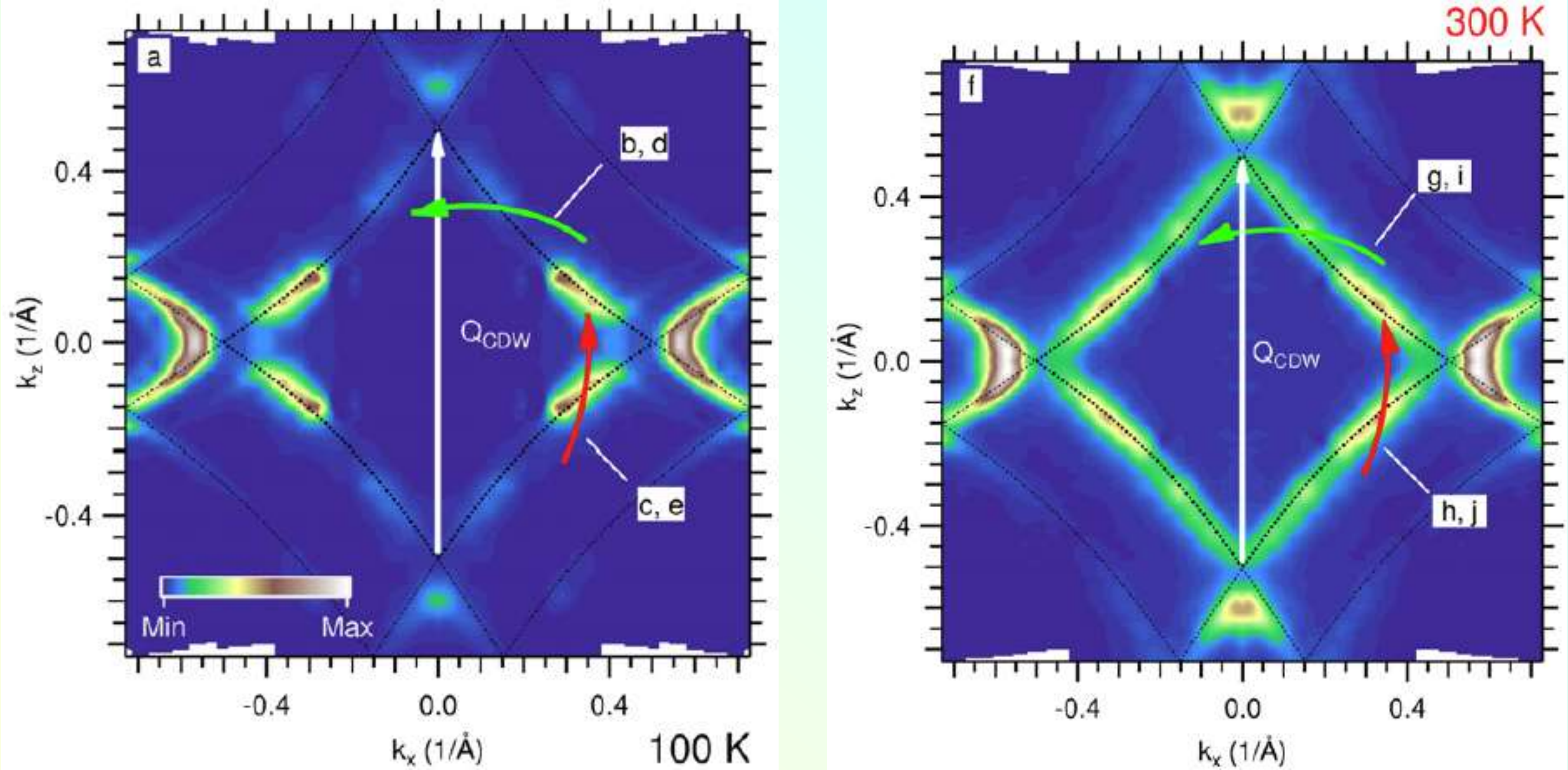

F. Schmitt et al., New Journal of Physics 13, 063022 (2011)

Momentum dependence of CDW energy gap

(determined from ARPES)

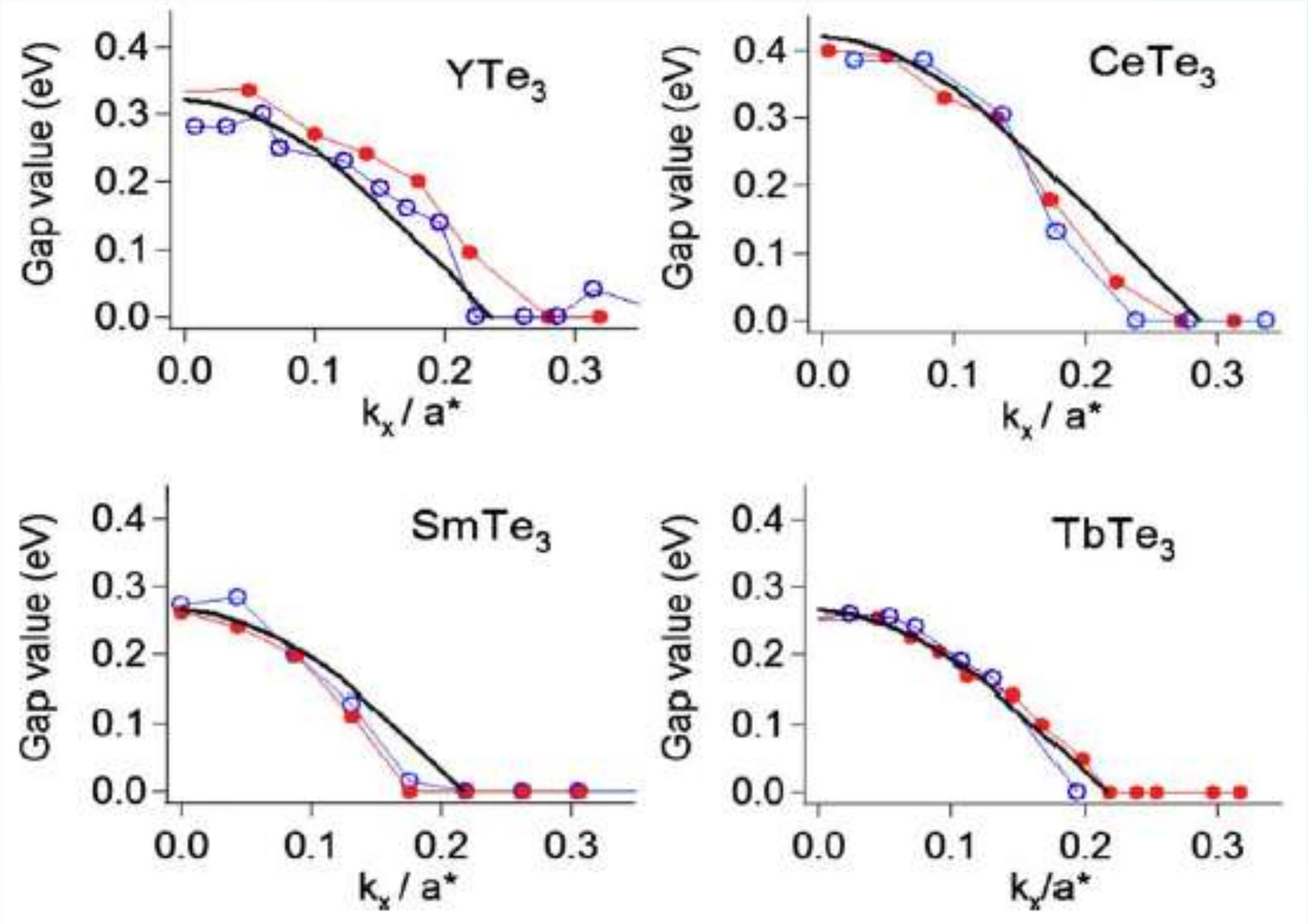

V. Brouet et al., Phys. Rev. B 77, 235104 (2008)

Electron dispersion and velocity.

Effect of momentum asymmetry of CDW gap.

Electron dispersion without CDW determined from band-structure calculations:

$$\varepsilon_1(k_x,k_y) = -2t_\parallel \cos[(k_x+k_y)a/2] - 2t_\perp \cos[(k_x-k_y)a/2] - E_F,$$

$$\varepsilon_2(k_x,k_y) = -2t_\parallel \cos[(k_x-k_y)a/2] - 2t_\perp \cos[(k_x+k_y)a/2] - E_F,$$

where $t_\parallel \approx 2$ eV, $t_\perp \approx 0.37$ eV

$E_F \approx 1.48$ eV and $a \approx 4.4 Å$ for $TbTe_3$

=>

The momentum dependence of electron velocity without CDW:

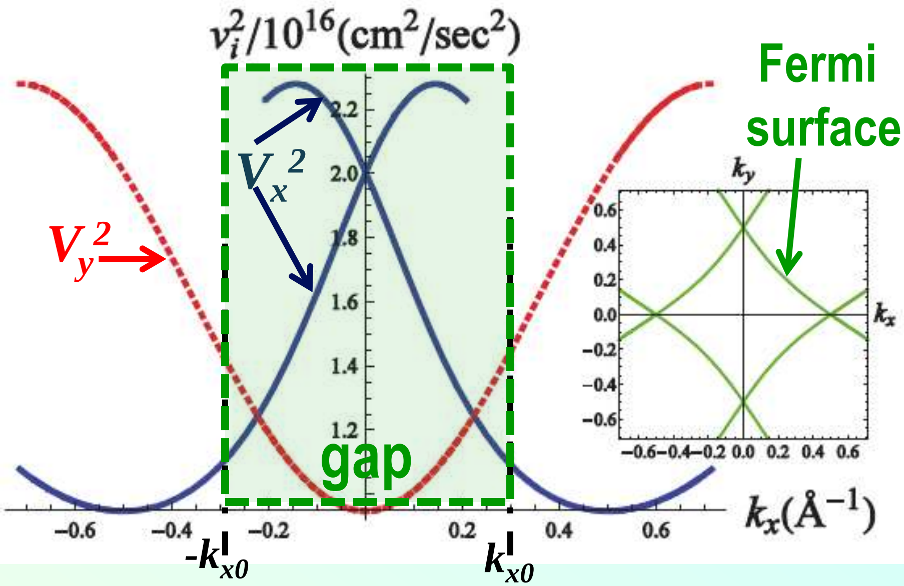

momentum asymmetry of CDW gap:

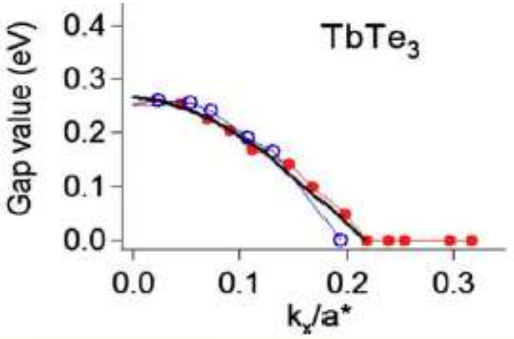

Electron conductivity: $\sigma_i(T) = 2e^2\tau \sum_{\boldsymbol{k}} v_i^2(\boldsymbol{k}) \left(-n_F'[\varepsilon(\boldsymbol{k})]\right)$

! CDW energy gap removes the electron states from FS parts with larger component $V_x^{\ 2}$, thus breaking the x-y isotropy of conductivity.

Results (1)

1. The anisotropy ratio depends strongly on $t_\perp / t_{||}$ in the electron dispersion without CDW. This can help to extract $t_\perp$ from experiment.

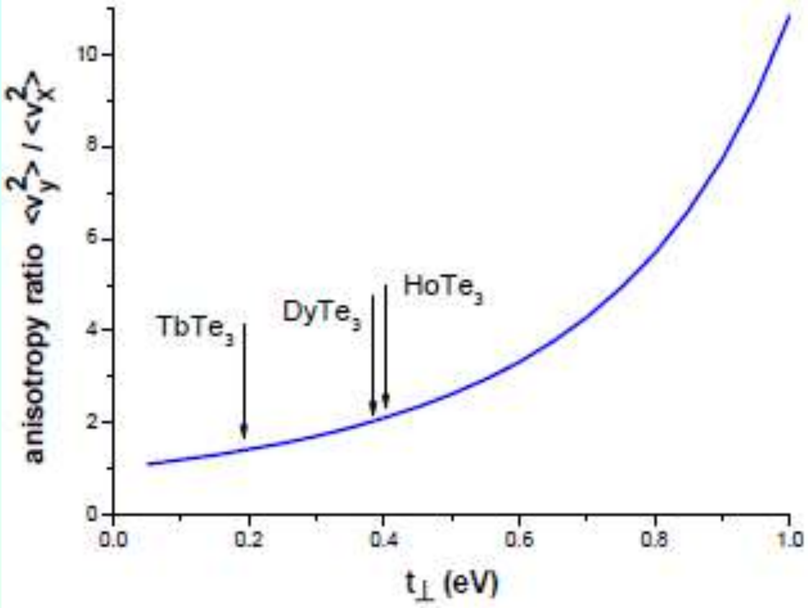

For RTe_3 where R=Tb,Dy,Ho,

with $t_{\|} \approx 2 \text{ eV}, \, t_{\perp} \approx 0.37 \text{ eV}$

and the calculated maximum anisotropy ratio (at T=0)

$$\frac{\sigma_{yy}}{\sigma_{xx}} \approx \frac{\int_{|k_x| \geq k_{x0}} dk_x \sqrt{1 + \left|\frac{dk_y}{dk_x}\right|^2_{FS}} v_y^2}{\int_{|k_x| \geq k_{x0}} dk_x \sqrt{1 + \left|\frac{dk_y}{dk_x}\right|^2_{FS}} v_x^2} \approx 1.96.$$

agrees with experiment, where this ratio ≈ 2

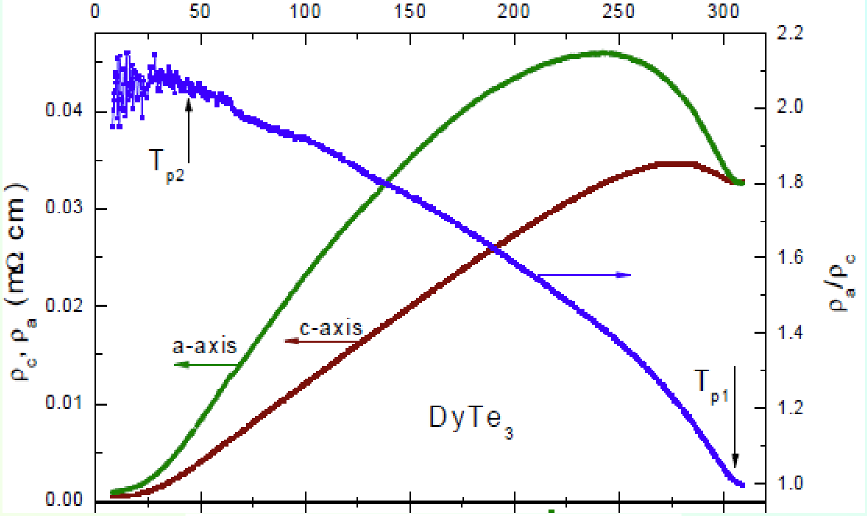

experimental data

Calculation of the temperature dependence of resistivity

Electronic conductivity in the τ-approximation: $\sigma_i(T) = 2e^2\tau \sum_{\boldsymbol{k}} v_i^2(\boldsymbol{k})\left(-n_F'\left[\varepsilon(\boldsymbol{k})\right]\right)$

CDW energy gap: $\Delta(T,\boldsymbol{k}) \approx \Delta_0(T)\,\Delta(\boldsymbol{k}) \approx \Delta_0(T)\left(1 - k_x^2/k_{x0}^2\right)$

$\Delta_0(T) \approx \Delta_0\left(1 - T^2/T_c^2\right)^\alpha, \ \alpha \geq 1/2.$

For $TbTe_3$ $\Delta_0 \approx 0.27\mathrm{eV}$ $k_{x0} \approx 0.29\text{Å}^{-1}$

Electron dispersion in the CDW state $E(\boldsymbol{k}) = \sqrt{\varepsilon^2(\boldsymbol{k}) + \Delta^2(T,\boldsymbol{k})}.$

Electron velocity:

$$v_{i\Delta}(\boldsymbol{k}) = \frac{\partial E(\boldsymbol{k})}{\partial k_i} \approx \frac{\varepsilon(\boldsymbol{k})\ \partial\varepsilon(\boldsymbol{k})/\partial k_i}{\sqrt{\varepsilon^2(\boldsymbol{k}) + \Delta^2(T,\boldsymbol{k})}} = v_i(\boldsymbol{k})\frac{\varepsilon(\boldsymbol{k})}{E(\boldsymbol{k})}.$$

Conductivity components

$$\sigma_i(T) = \frac{e^2\rho_F\tau}{d}\int_{-\pi/a}^{\pi/a}\frac{a\,dk_x}{2\pi}\sqrt{1+\left(\frac{dk_y}{dk_x}\right)^2}v_i^2(k_x) \times \int \frac{d\varepsilon}{v_F}\frac{-n_F'\left[\sqrt{\varepsilon^2+\Delta^2(T,k_x)}\right]\varepsilon^2}{\varepsilon^2+\Delta^2(T,k_x)},$$

where $\varepsilon(\boldsymbol{k})$ is the electron dispersion without CDW

Results (2)

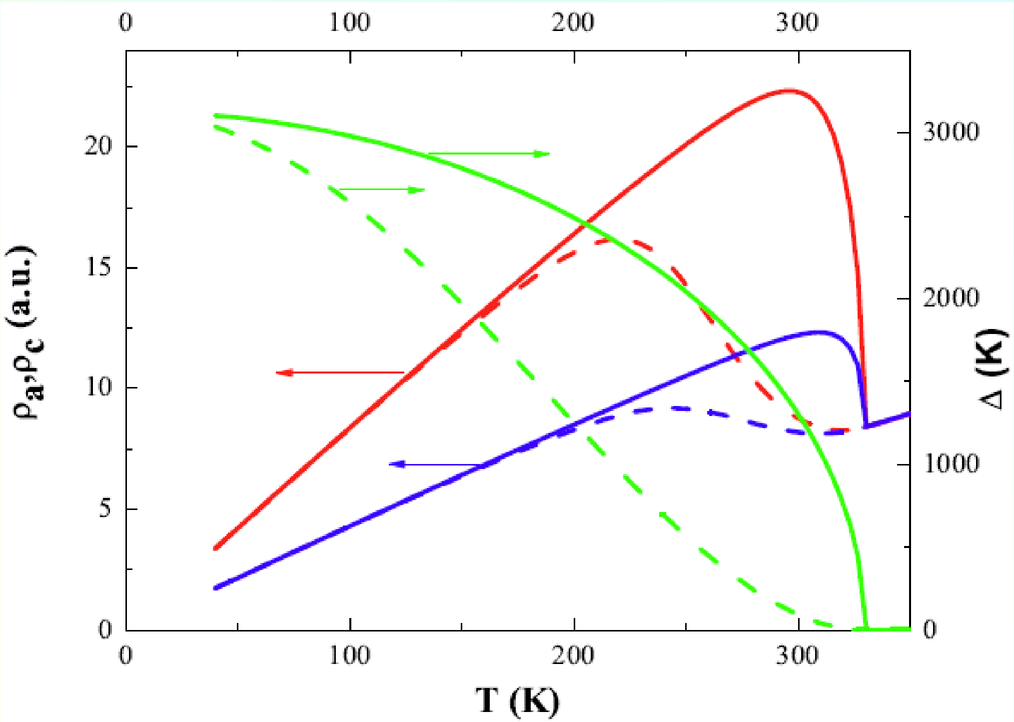

FIG. 6: (color online) The calculated temperature dependence of resistivity $\rho_a = 1/\sigma_{xx}$ solid (dashed) red lines and $\rho_c = 1/\sigma_{yy}$ solid (dashed) blue lines in the presence of CDW

2. Temperature dependence of various conductivity components is sensitive to the T-dependence of CDW gap Δ(T), determined by fluctuations. This allows to compare various theoretical predictions of Δ(T) with experiment.
It best agrees well with experiment for α≈1.5 .

temperature dependence of CDW gap is given by

$$\Delta_0(T) \approx \Delta_0 \left(1 - T^2/T_c^2\right)^{\alpha}, \; \alpha \geq 1/2.$$

with α=1/2 (solid green line) and α=2 (dashed green)

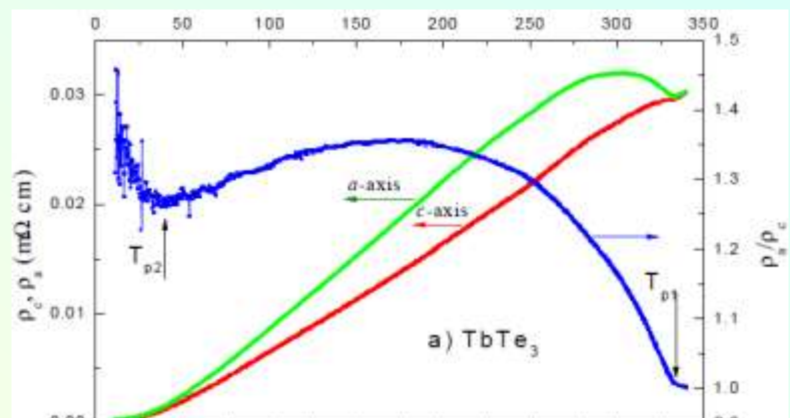

Sub-Conclusion (of Part 1)

1. The quasi-isotropic conductivity in the normal state of untwinned RTe_3 compounds is broken by the CDW gap appearing below T_{CDW}

2. We explain it by the momentum-dependent CDW gap. It removes the electron states from FS parts with larger component V_x^2, thus breaking the x-y isotropy of conductivity.

3. The performed calculations of conductivity in the τ-approximation with electron dispersion modified by the momentum-dependent CDW gap (determined from ARPES) agrees well with experimental data on conductivity in various RTe_3 compounds.

4. This allows to specify the electron dispersion parameter $t_\perp$ and the temperature dependence of CDW gap close to T_c

5. Similar calculation allows to obtain information about the momentum dependence of the CDW/SDW energy gap even if ARPES data are not available

Part 2

New scattering mechanism of electrons in the partial density-wave state in magnetic field

Main message:

In the density-wave state conserving metallic conductivity magnetoresistance (MR) studies must take into account the new scattering mechanism of conducting electrons, coming from the non-uniform magnetic breakdown.
It leads to the increase of longitudinal MR and (sometimes in quasi-2D materials) to the phase inversion of MQO.
This mechanism can be much stronger than impurities.

Magnetoresistance studies of organic metals

There are very many papers on the study of electronic properties of organic metals using magnetoresistance measurements.

Some books:
1. J. Wosnitza, *Fermi Surfaces of Low-Dimensional Organic Metals and Superconductors* (Springer-Verlag, Berlin, 1996).
2. T. Ishiguro, K. Yamaji, and G. Saito, *Organic Superconductors*, 2nd ed. (Springer-Verlag, Berlin, 1998).
3. A.G. Lebed (ed.), *The Physics of Organic Superconductors and Conductors*, (Springer Series in Materials Science, 2009).

Some review papers:
1. **D. Jérome and H.J. Schulz, Adv. Phys. 31, 299 (1982).**
2. **J. Singleton, Rep. Prog. Phys. 63, 1111 (2000).**
3. **M.V. Kartsovnik, *High Magnetic Fields: A Tool for Studying Electronic Properties of Layered Organic Metals*, Chem. Rev. 104, 5737 (2004).**
4. **M.V. Kartsovnik , V.G. Peschansky, *Galvanomagnetic Phenomena in Layered Organic Conductors*, FNT 31, 249 (2005) [LTP 31, 185].**

Angular dependence of background magnetoresistance

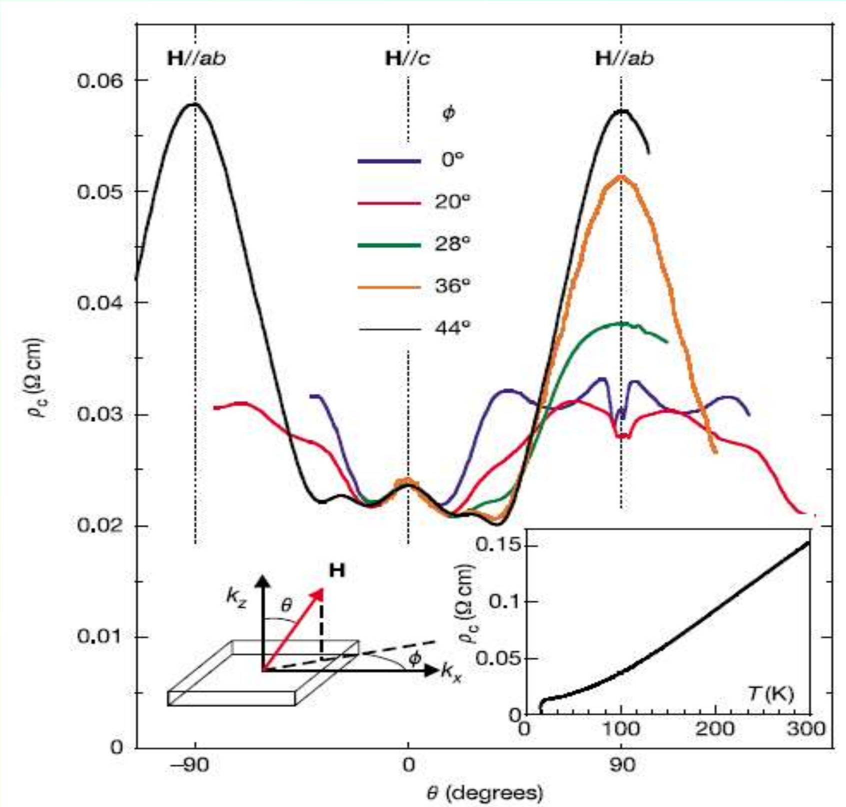

Figure 1 Polar AMRO sweeps in an overdoped Tl2201 single crystal ($T_c \approx 20$ K). The data were taken at $T = 4.2$ K and $H = 45$ T. The different azimuthal orientations ($\pm 4°$) of each polar sweep are stated relative to the Cu–O–Cu bond direction. The key features of the data are as follows: (1) a sharp dip in $\rho_\perp$ at $\theta = 90°$ for low values of ϕ, which we attribute to the onset of superconductivity at angles where $H_{c2}(\phi, \theta)$ is maximal, (2) a broad peak around **H**||ab ($\theta = 90°$) that is maximal for $\phi \approx 45°$, consistent with previous azimuthal AMRO studies in overdoped Tl2201 (ref. 16), (3) a small peak at **H**||c ($\theta = 0°$), and (4) a second peak in the range $25° < \theta < 45°$ whose position and intensity vary strongly with ϕ. These last two features are the most critical for our analysis. Similar

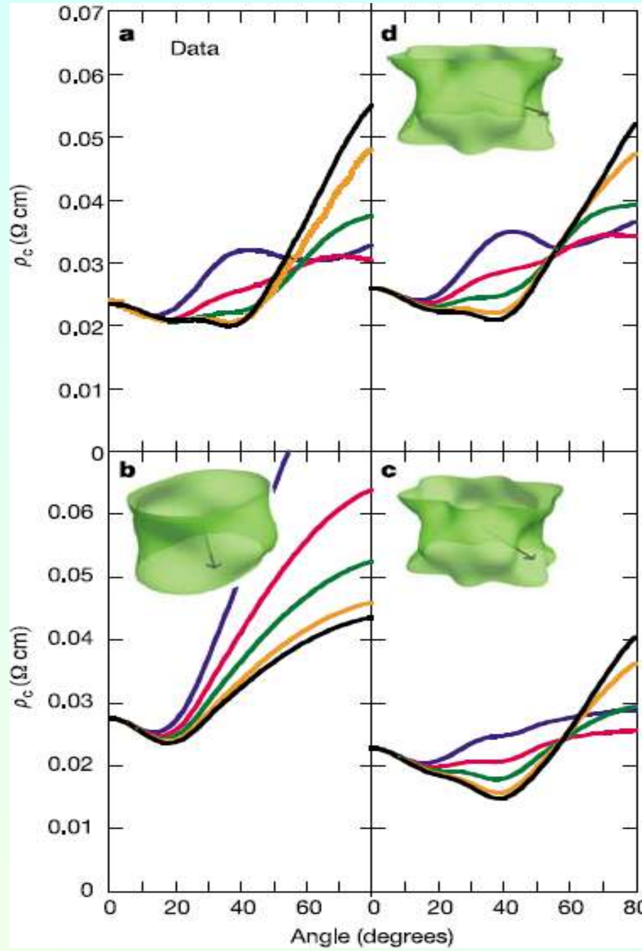

Reconstruction of the FS in $Tl_2Ba_2CuO_{6+d}$ from polar AMRO data.

N. E. Hussey et al., "A coherent 3D Fermi surface in a high-Tc superconductor" Nature 425, 814 (2003)

AMRO experiment proved (for the first time) the existence of Fermi surface in cuprate high-Tc superconductors

Strong and weak points of magnetoresistance as a tool to study electronic properties

Strong point: high precision and availability

Weak point: requires reliable theoretical description

Therefore, any unusual/unexpected qualitative feature must be analyzed and understood

Experimental facts and motivation

Magnetoresistance in layered organic metal α-(BEDT-TTF)$_2$MHg(SCN)$_4$, (M=K,Tl,Rb,..)

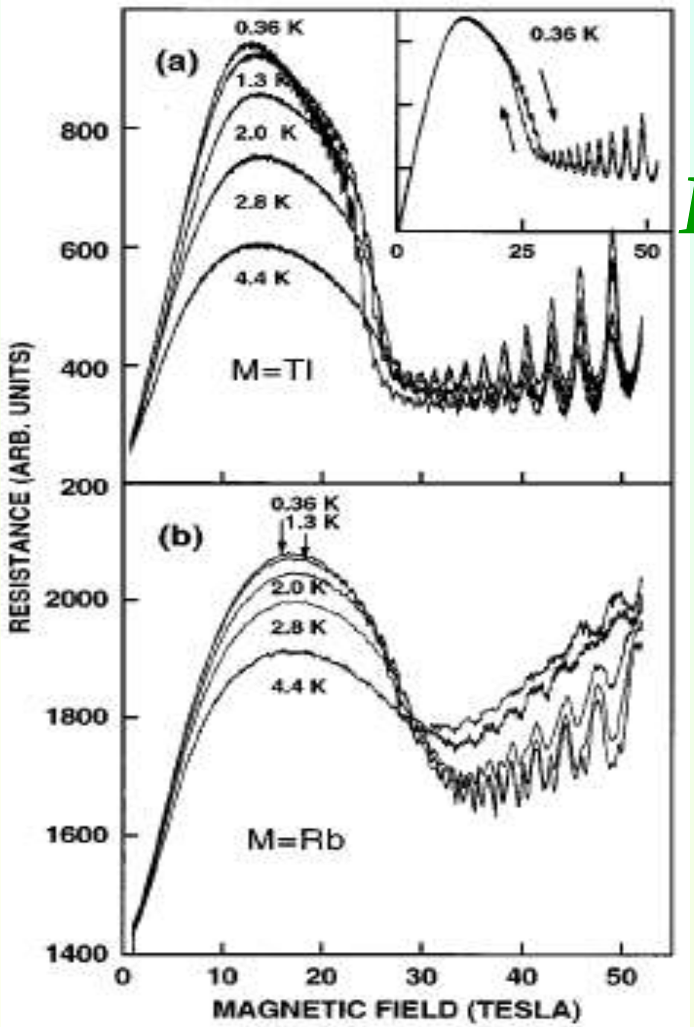

R.H. McKenzie et al., PRB 54, R8289 (1996)

$B \parallel I \parallel z$

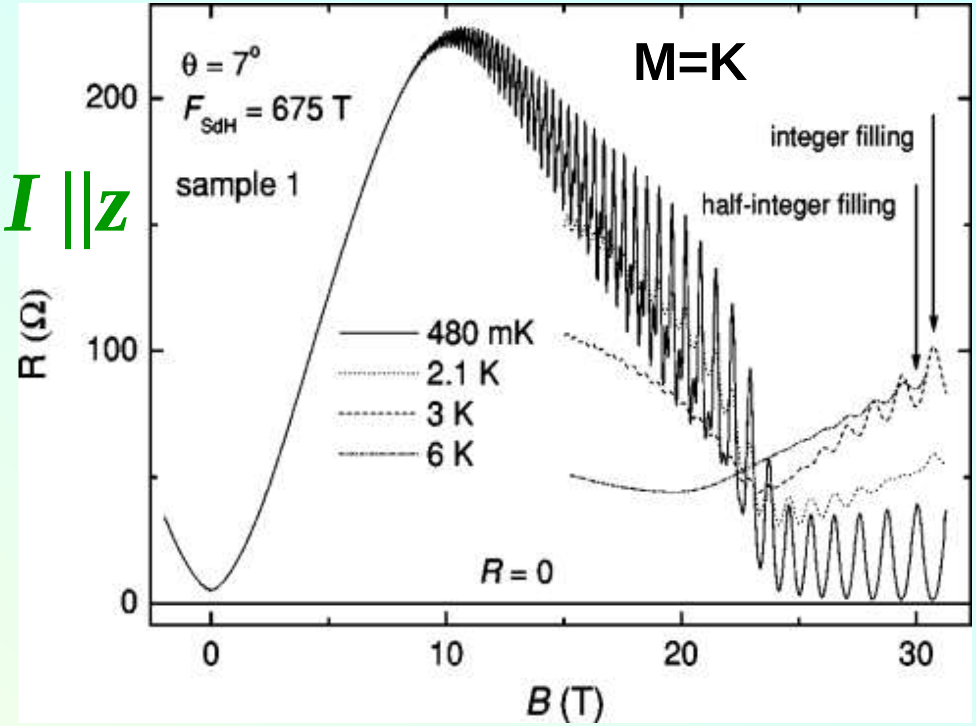

N. Harrison et al., PRB 62, 14 212 (2000)

Importnant experimental facts:

1. Hump on MR at B~12T
2. Phase inversion of Shubnikov - de Haas oscillations in CDW

Example 2

Magnetoresistance in layered organic metals α-(BEDT-TTF)$_2$MHg(SCN)$_4$, (M=K,Tl,Rb,..)

Phase diagram of α-(BEDT-TTF)$_2$KHg(SCN)$_4$

High magnetic field destroys CDW_0 by the Zeeman splitting and the non-uniform CDW_x is formed at $B>B_c$ with lower T_c :

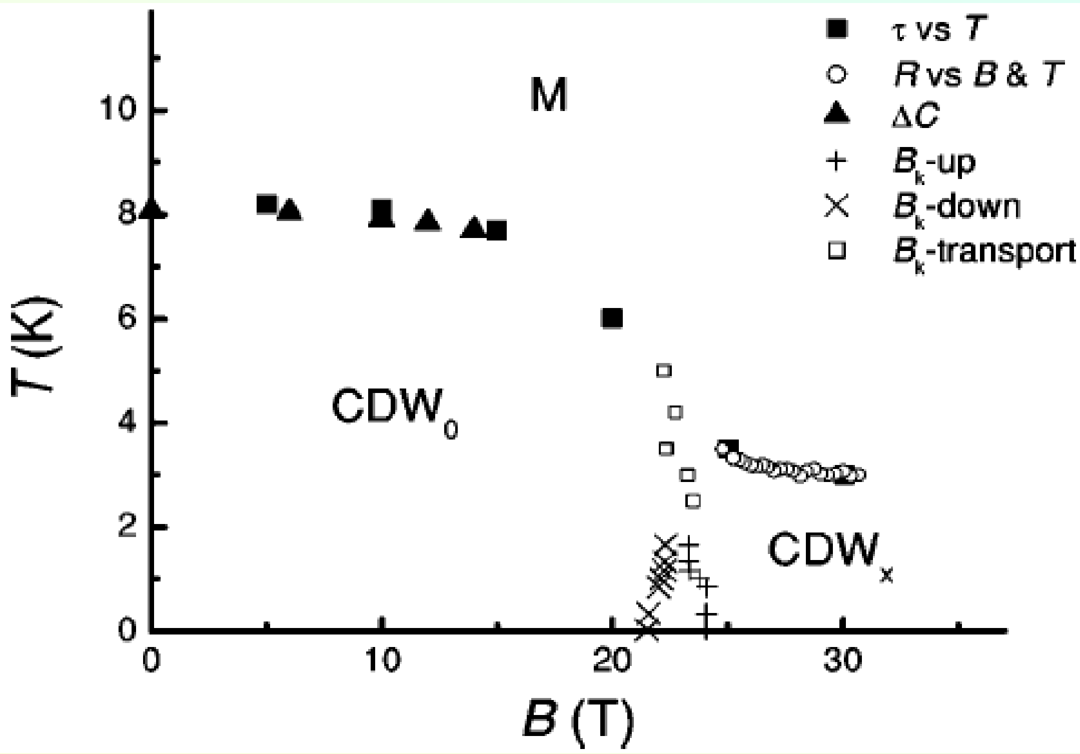

N. Harrison et al., PRB 62, 14212 (2000)

Pressure also damps CDW:

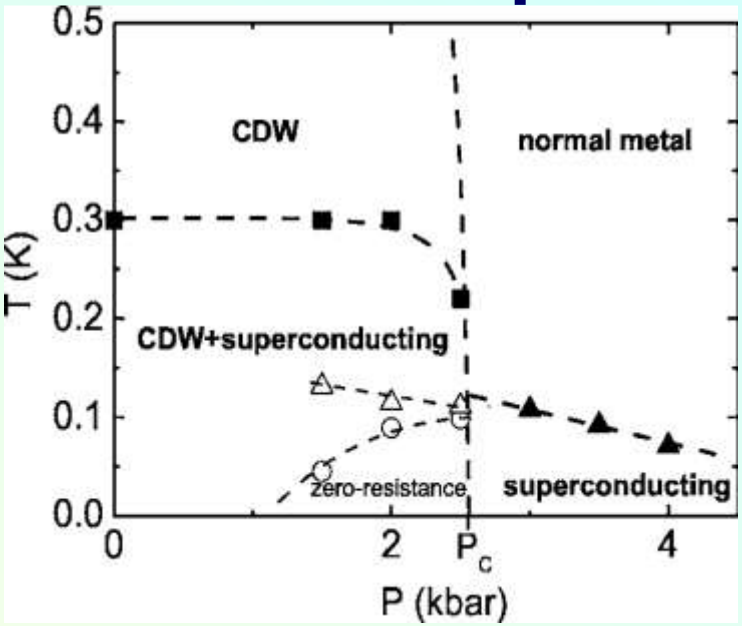

D. Andres et al., PRB 72, 174513 (2005)

Phase diagram of α-(BEDT-TTF)$_2$KHg(SCN)$_4$ and the line of phase inversion of MQO

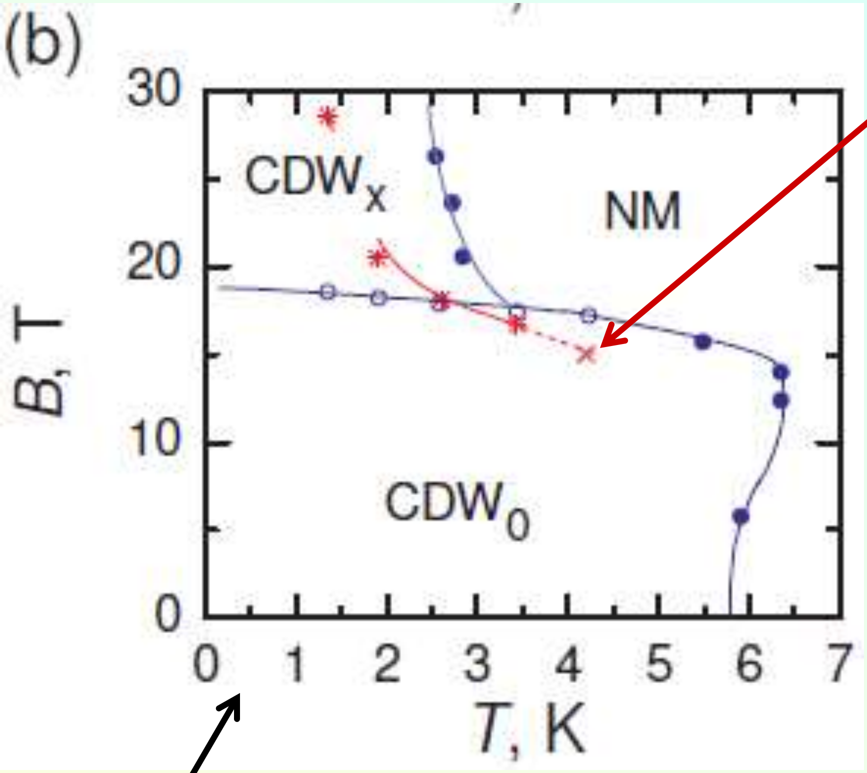

The phase inversion points * follow the CDW transition line

This suggest that the phase inversion of MQO is related to CDW transition, to CDW energy gap or to FS reconstruction

However, this phase inversion remained puzzling for decades

Ref: M.V. Kartsovnik, V.N. Zverev, D.Andres, W.Biberacher, T.Helm, P.D. Grigoriev, R.Ramazashvili, N.D. Kushch, H.Muller, Low Temp. Phys. 40(4), 377 (2014) [FNT 40(4), 484]; arXiv:1311.5744.

Phase inversion of Shubnikov –de Haas oscillations

Experimental data. The phase inversion is in the dashed region of B-T

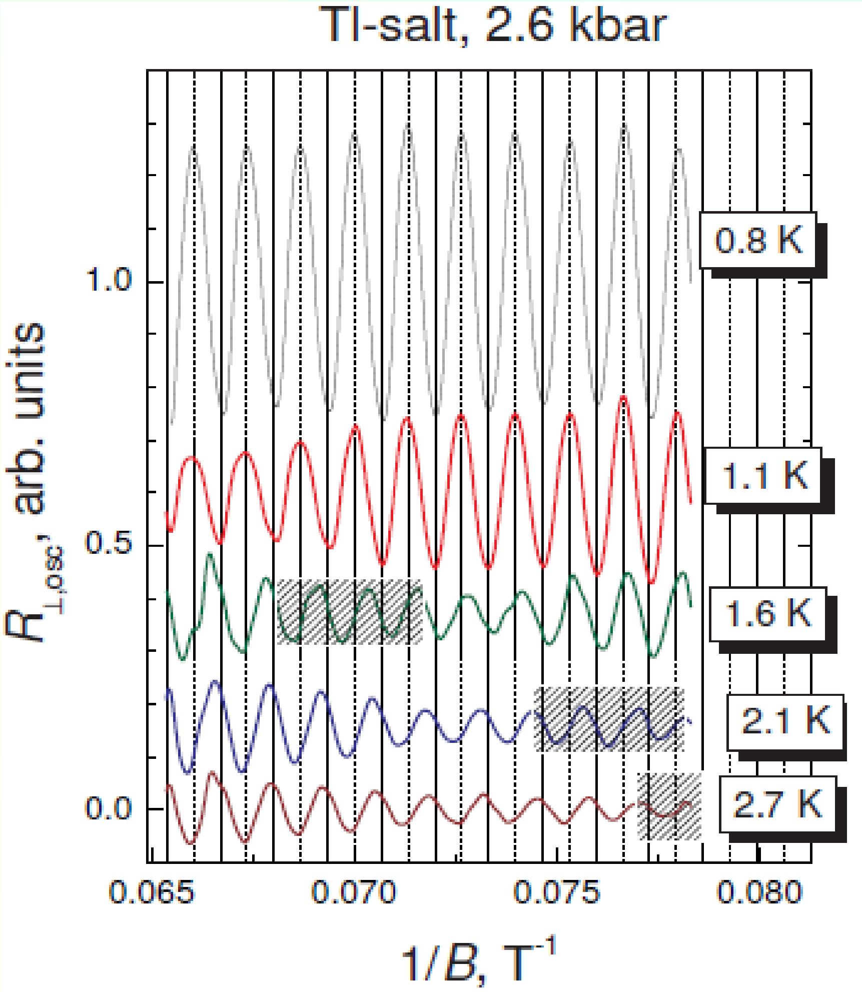

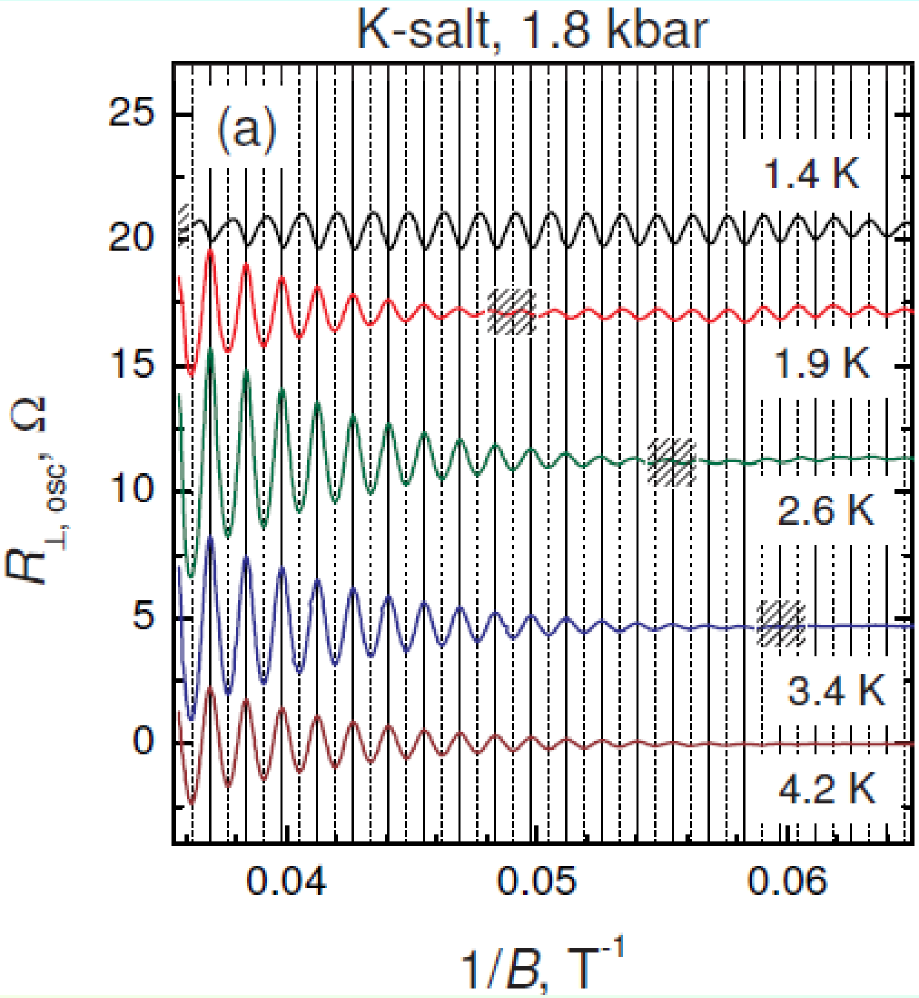

Low Temp. Phys., 40(4), 377-383 (2014) [arXiv:1311.5744]

Origin of magnetic quantum oscillations in metals

For parabolic electron dispersion in zero magnetic field
$\varepsilon(p)= p_x^2/2m_x + p_y^2/2m_y + p_z^2/2m_z$,

in magnetic field directed along z-axis the dispersion relation is
$\varepsilon(n,p_z)=\hbar\omega_c(n+1/2)+p_z^2/2m_z$,
where $\omega_c=eB/mc$
(Landau level quantization).

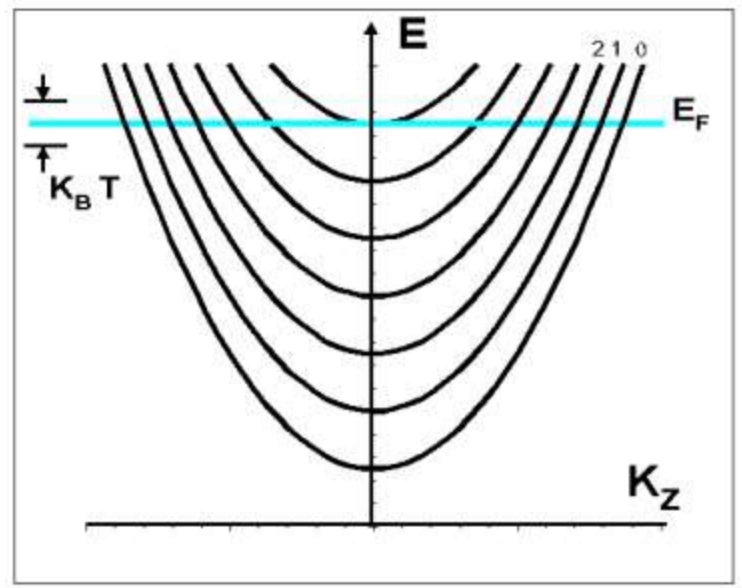

As the magnetic field increases the Landau levels periodically cross Fermi level.

This results in magnetic quantum oscillations (MQO) of thermodynamic (DoS, magnetization) and transport electronic properties of metals.

In 3D the DoS oscillations are weak, because the integration over p_z smears them out.

In 2D the DoS oscillations can be strong and sharp, leading to the sharp and non-sinusoidal MQO.

Shubnikov – de Haas oscillations in 3D and 2D metals

MQO of conductivity in 3D metals mainly come from the oscillations of electron mean free time $\tau \sim 1/\rho(E_F)$. The DoS $\rho(E_F)$ oscillates because of Landau level quantization.

$$\sigma_{zz}^{3D} = e^2 \tau \sum_{FS} v_z^2 ,$$

where in the Born approximation the scattering rate is given by golden Fermi rule:

$$1/\tau = \frac{2\pi}{\hbar} n_i |v|^2 \boxed{\int dp_z \sum_n \delta(\varepsilon(n,\ p_z) - \mu) \frac{eH/c}{(2\pi\hbar)^2}}.$$

DoS

So, in 3D conductivity is inversely proportional to the DoS,

because oscillations of scattering rate 1/τ dominate oscillations of mean square electron velocity averaged over FS.

In 2D maxima of conductivity coincide with DoS maxima,

because between the LLs there is no electron states to conduct =>

the phase of Shubnikov-de Haas oscillations in 2D and 3D differs by π

⇒2D and 3D cases are not described by the same formula!

⇒There is a phase inversion as we go from 3D to 2D case.

Fermi surface reconstruction by CDW

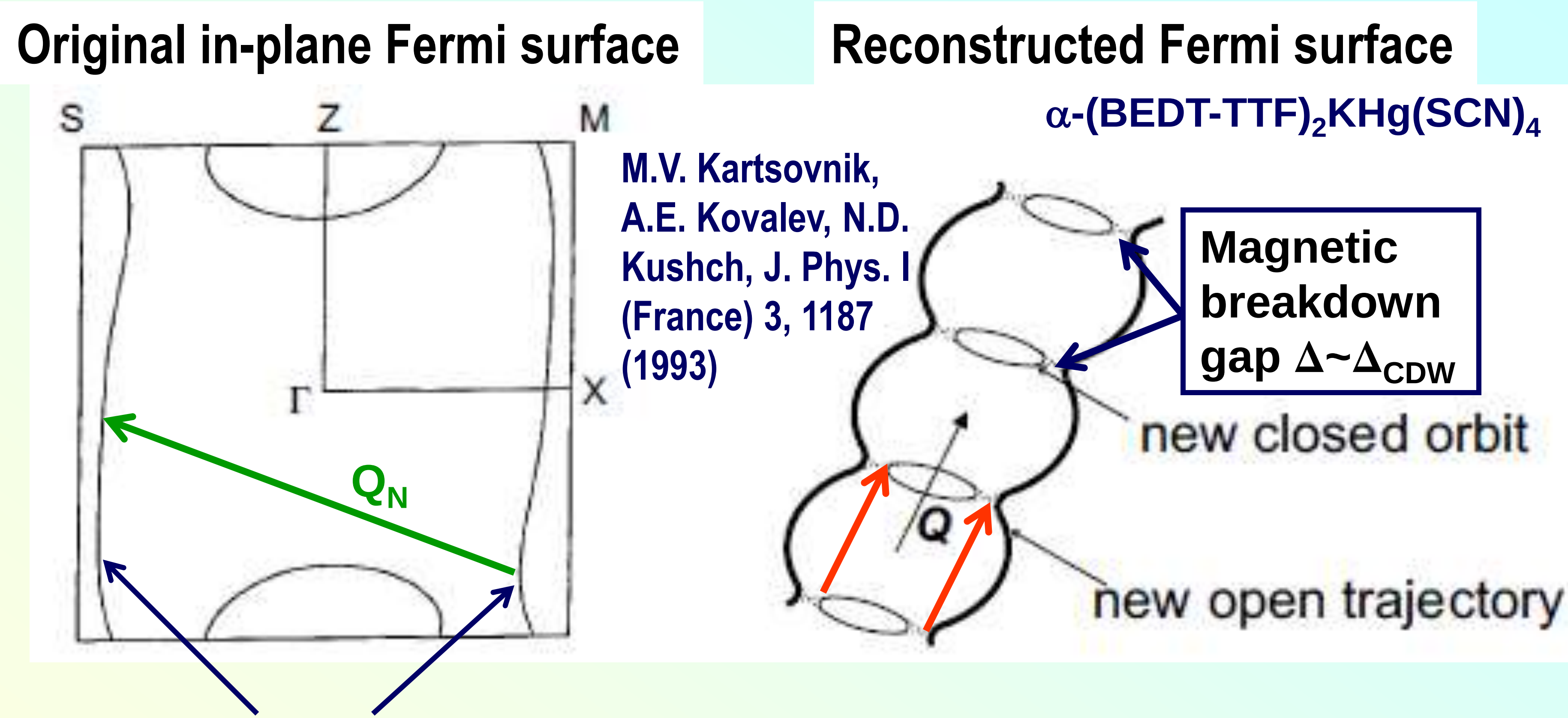

The quasi-1D FS parts possess nesting property with vector Q and become gapped in the CDW state. The CDW creates periodic potential and the new Brillouin zone. The quasi-2D FS pockets then overlap and form reconstructed FS with new quasi-1D sheets and small 2D pockets.

Even 2D FS pockets, having no nesting property, become reconstructed by CDW on 1D parts!

The observed MQO support this FS reconstruction

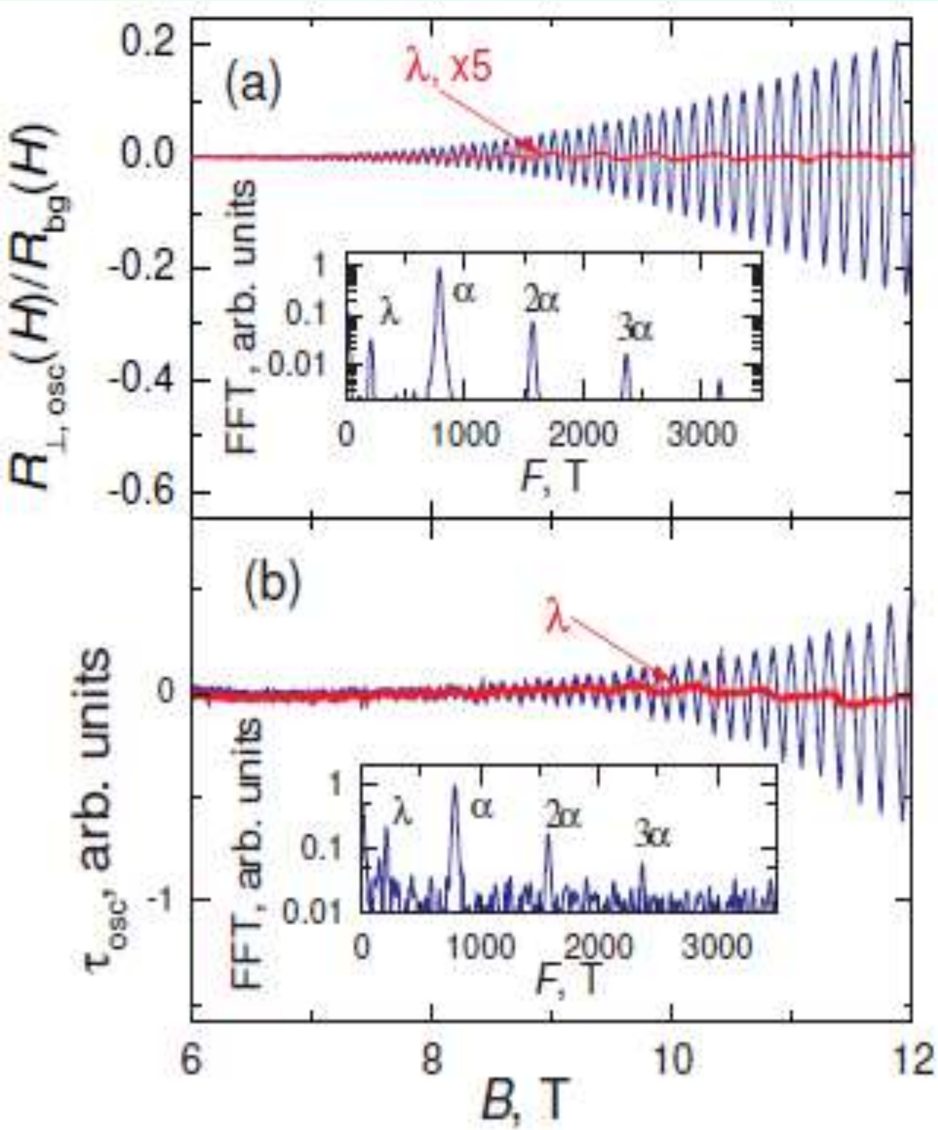

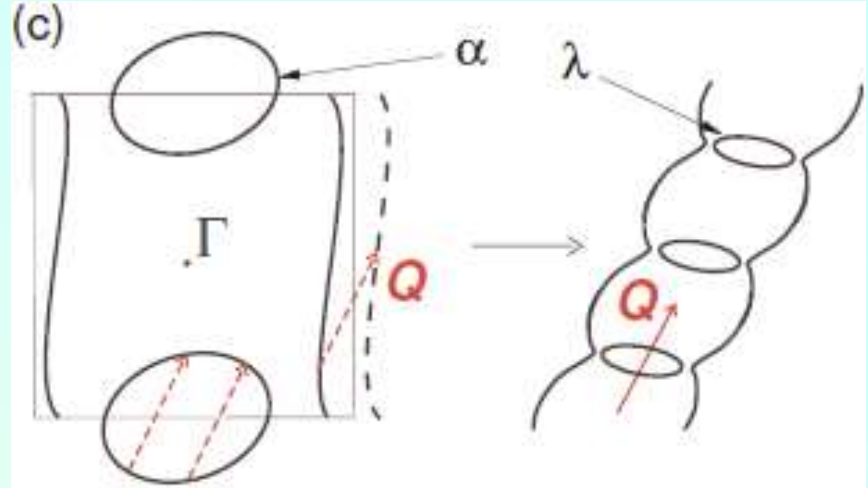

Figure 2. Oscillating components of the magnetoresistance (a) and magnetic torque (b) of the K-salt at $T = 0.45\,\mathrm{K}$, $\theta = 31.5^\circ$. The red curves are obtained by filtering out the α-oscillations and demonstrate the behavior of the slow oscillations with frequency $F_\lambda = 210\,\mathrm{T}$. In (a) the λ-oscillations are magnified by a factor of 5, for a better visibility. The insets in (a) and (b) show the corresponding fast Fourier spectra. (c) Schematic 2D view of the Fermi surface reconstruction due to the CDW potential with the wave vector Q. The original Fermi surface (left panel) consists of a pair of open sheets and a cylinder. The CDW, introducing a new periodicity with the wave vector Q, opens a gap at the Fermi level in the whole q1D band as well as in the q2D band at the states separated by Q (right panel).

M.V. Kartsovnik, V.N. Zverev, .. , P.D. Grigoriev, R.Ramazashvili, N.D. Kushch, H.Muller, Low Temp. Phys., 40(4), 377 (2014) [FNT 40(4), 484]; arXiv:1311.5744

FS reconstruction in high-Tc cuprates (just another example)

$Nd_{2-x}Ce_xCuO_4$

(NCCO)

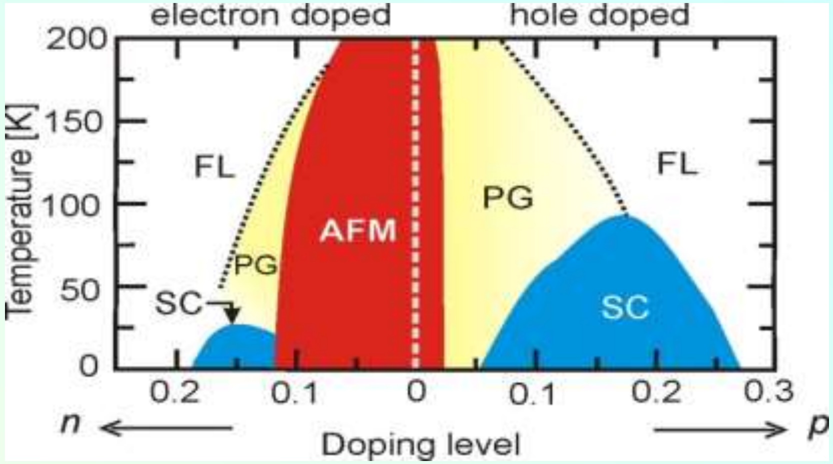

! The Fermi-surface reconstruction is <u>very common</u> and can be easily seen by MQO

Original FS:

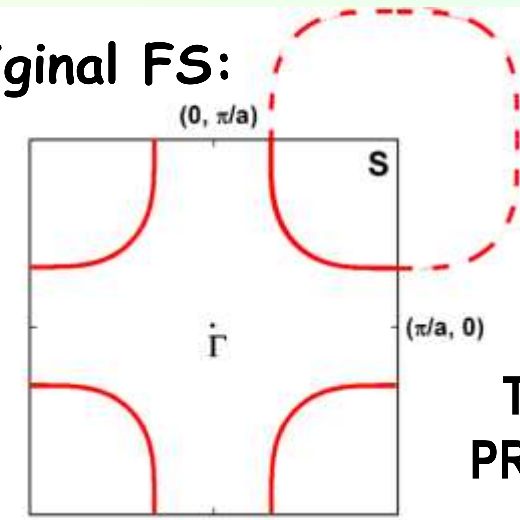

<u>n = 0.17</u>

S_h = 41.5% of S_{BZ}

T. Helm et al., PRL 103, 157002 (2009)

Reconstructed FS:

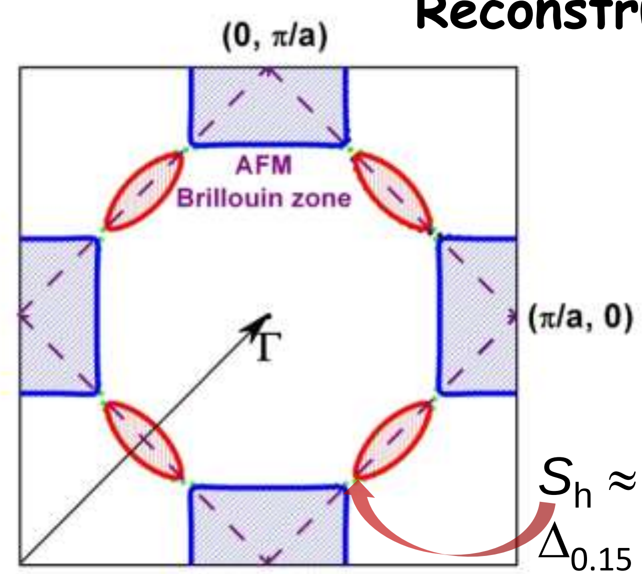

<u>n = 0.15 and 0.16</u>

$S_h \approx$ 1.1% of S_{BZ};

$\Delta_{0.15} \approx$ 64 meV;

$\Delta_{0.16} \approx$ 36 meV

Reconstruction of FS is weak, but the electron trajectories strongly change in the momentum space

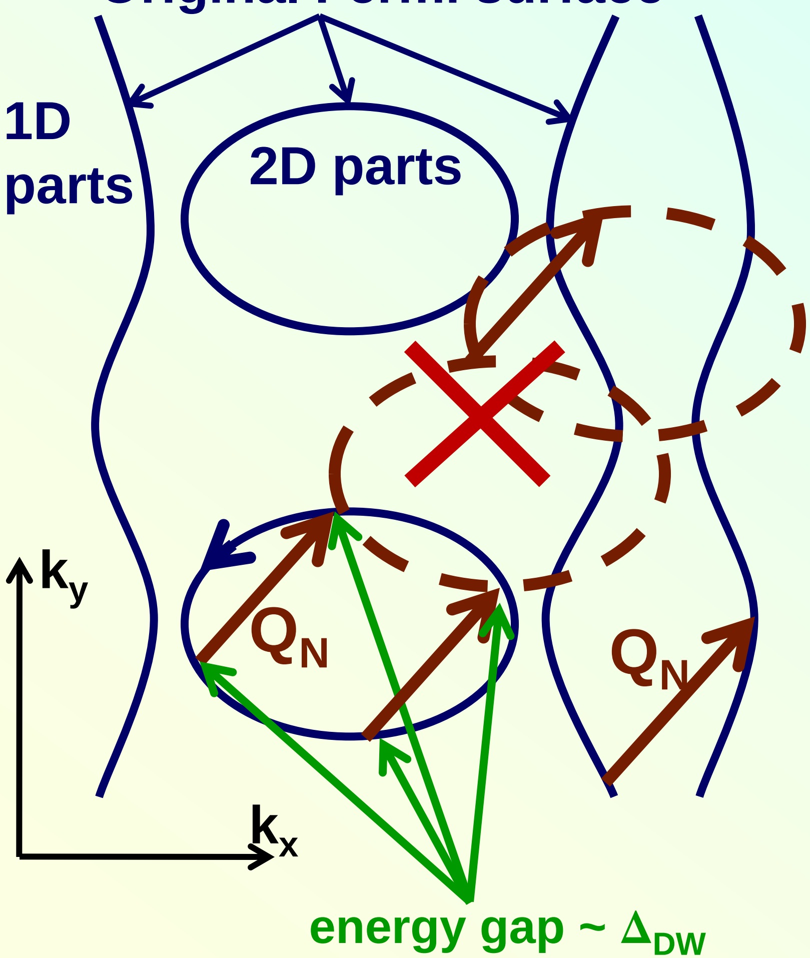

No additional parts of FS are created by density wave!

Only small energy gap is formed at the boundaries of new Brillouin zone However, this gap strongly changes the electron trajectories, e.g., from closed (2D) to open (1D).

The electrons just scatter by Q_N to the same FS part.

Even electron trajectories from 2D FS pockets, having no nesting property, become reconstructed by CDW to open 1D trajectories!

Theory of magnetic breakdown (MB)

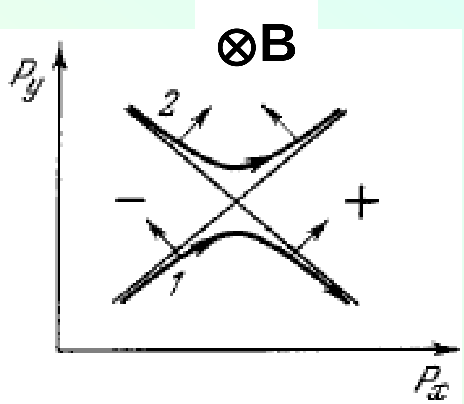

The 2D scattering matrix between the states 1 and 2

$$\hat{S} = \begin{pmatrix} \sqrt{1-W}\, e^{i\Lambda}, & -\sqrt{W} \\ \sqrt{W}, & \sqrt{1-W}\, e^{-i\Lambda} \end{pmatrix}$$

where the MB probability $W = \exp\{-H_0/H\}$

the MB field $H_0 \sim \Delta^2/E_F$ **is much smaller than gap!**

$(\, B_{MB} \sim \Delta^2 m_c/\hbar e E_F \,)$ **The MB phase** $\Lambda = \dfrac{\pi}{4} + \dfrac{H_0}{\pi H} - \dfrac{H_0}{\pi H} \ln \dfrac{H_0}{\pi H} + \arg \Gamma\left(i \dfrac{H_0}{\pi H}\right)$

Remark: the MB field H_0 can be calculated with coefficient:

If one takes the electron dispersion at the MB point in a general form as

$$\varepsilon_{1,2}(p) = \varepsilon_M + v_M\, \delta p_n + \sqrt{\Delta^2/4 + (v^M_{1,2}\, \delta p_n)^2}\,,$$

$$\varepsilon_M = \tfrac{1}{2}[\varepsilon_1(p_M) + \varepsilon_2(p_m)]\,, \quad \delta p_n = n_M(p - p_M)$$

$$v_M = \tfrac{1}{2}(v^M_{11} + v^M_{22})\,, \quad \Delta = \Delta(p_M) = \varepsilon_1(p_M) - \varepsilon_2(p_M)\,;$$

The MB field H_0 then

$$H_0 = \frac{c\pi\Delta^2}{e\hbar\, |v_x v_{12} \cos\theta|}$$

M.I. Kaganov, A.A. Slutskin, Phys. Reports 98, 189 (1983)

Idea:

Origin of MB scattering mechanism

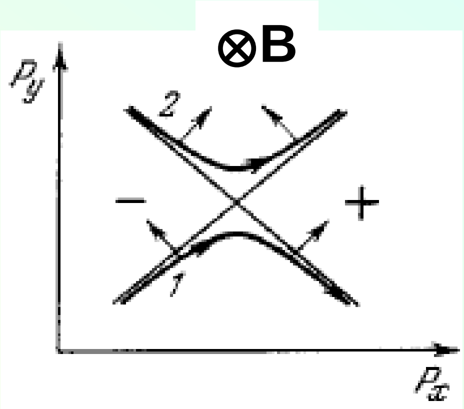

The 2D scattering matrix between the states 1 and 2

$$\hat{S} = \begin{pmatrix} \sqrt{1-W}\,e^{i\Lambda}, & -\sqrt{W} \\ \sqrt{W}, & \sqrt{1-W}\,e^{-i\Lambda} \end{pmatrix}$$

where the MB probability $W = \exp\{-H_0/H\}$

the MB field $H_0 \propto \Delta^2/E_F$ is << DW gap!

Uniform MB, though strongly scatters conducting electrons, does not lead to the momentum relaxation along field because does not break the spatial uniformity (which gives momentum conservation).

Idea: non-uniform MB may give the electron momentum relaxation!

If a local MB defect scatters an electron differently from uniform MB, it also changes electron momentum along magnetic field => **new scattering mechanism**

The weak spatial fluctuations of CDW gap Δ (or DW defects or solitons) result to strong fluctuations of the MB probability (due to FS reconstruction).

MB defects are not scattering potential, but variations of scattering matrix. They are strong because corresponding change of MB probability is ~1

Local change of MB probability as a scattering center for conducting electrons

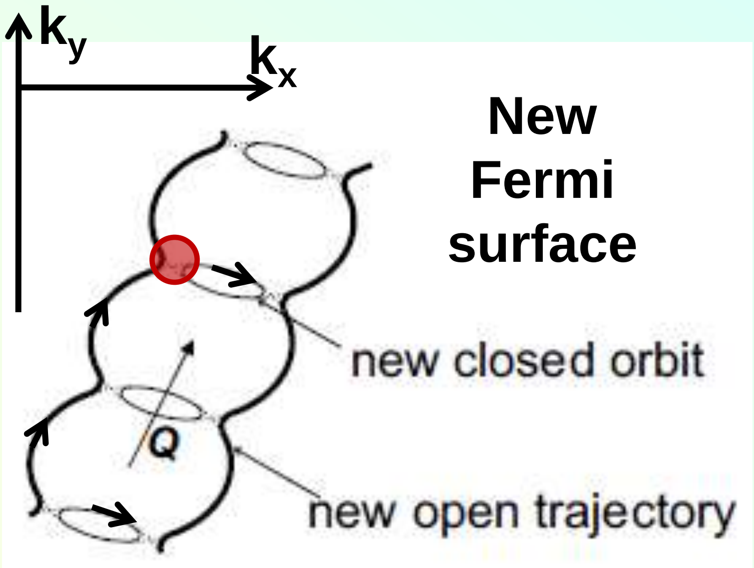

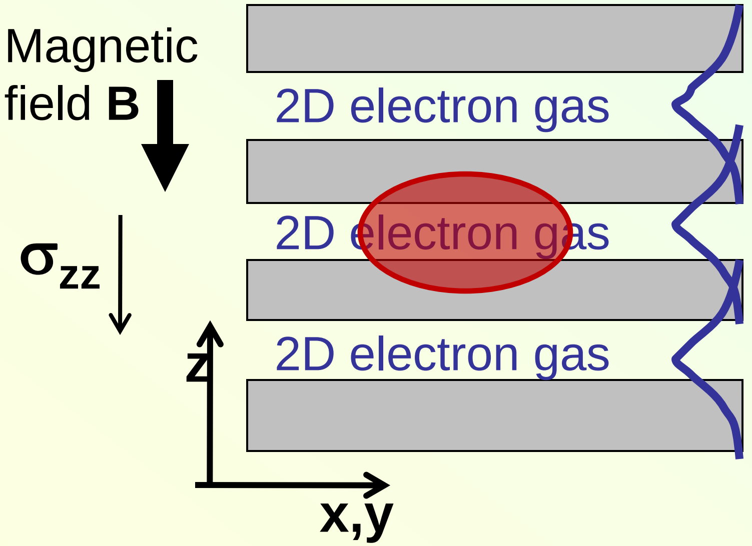

New electron spectrum contains two types of electron states or 2 bands:

1) **non-quantized quasi-1D states**
2) **2D states, giving Landau levels**

The scattering from normal impurities to all states at the same energy is $\propto \rho_{tot}$

Assume the MB probability W≅0 everywhere except the MB defect spots (red), where W≅1. And these defects are localized in z-direction, so that they scatter to any p_z. Then they act as scattering centers!

The MB defects scatter electrons between the two bands 1D ↔ 2D

Phase inversion of Shubnikov –de Haas oscillations

The phase inversion comes because the MB scattering is non-diagonal between the FS parts (or, the electron spectrum parts). The defects, increasing the MB amplitude (local reduction of the DW gap), scatter mainly to 2D parts (quantized electron spectrum): $1/\tau_{\mathrm{MB}} \propto \rho_{2D}\left(E_{\mathrm{F}}\right)$

In τ–approximation electron conductivity

$$\sigma_{zz} = 2e^2\tau_{tot}\sum_{\boldsymbol{k}} v_z^2\left(\boldsymbol{k}\right)\left(-n_F'\left[\varepsilon_{1D}\left(\boldsymbol{k}\right)\right]\right)$$

where the total scattering rate is a sum of MB and impurity contributions:

$$1/\tau_{tot} = 1/\tau_{\mathrm{MB}} + 1/\tau_i$$

When both 1D and 2D parts

$$\sigma_{zz} \propto \frac{\left\langle v_{z1D}^2\right\rangle \rho_{1D}\left(E_{\mathrm{F}}\right) + \left\langle v_{z2D}^2\right\rangle \rho_{2D}\left(E_{\mathrm{F}}\right)}{\rho_{2D}\left(E_{\mathrm{F}}\right)}.$$

$$\left\langle v_{z\,2D}^2\right\rangle(\epsilon) \approx \left\langle v_{z\,1D}^2\right\rangle\left[1 - 2\alpha R_D\cos\left(2\pi\epsilon/\hbar\omega_c\right)\right], \quad \left\langle v_{z\,1D}^2\right\rangle \approx 2t_\perp^2 d^2/\hbar^2$$

The conductivity

$$\boxed{\sigma_{zz} \propto const + \left(\frac{\rho_{1D0}}{\rho_{2D0}} - \alpha\right) 2R_D\cos\left(2\pi F/B\right)}$$

The MQO amplitude changes sign !

Magnetoresistance in layered organic metal α-(BEDT-TTF)$_2$MHg(SCN)$_4$, (M=K,Tl,Rb,..)

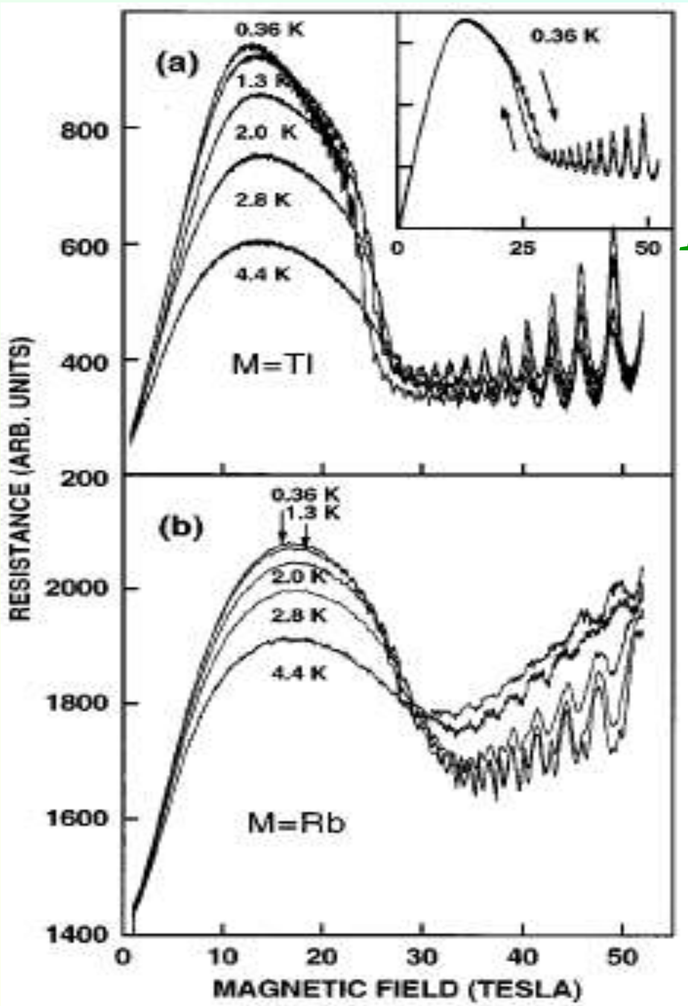

R.H. McKenzie et al., PRB 54, R8289 (1996)

$B \parallel I \parallel z$

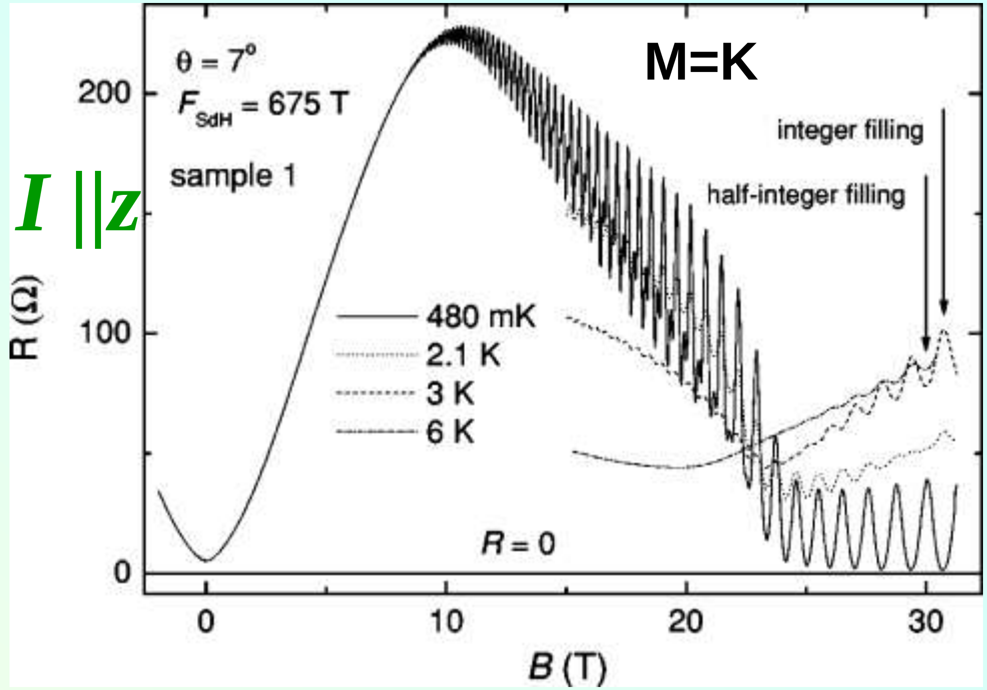

N. Harrison et al., PRB 62, 14 212 (2000)

The observed increase of MR at B~5-20T~H_0 may be due to this new scattering mechanism on MB defects

This mechanism is rather general !

Increased resistivity at MB field H_0 shows the CDW defects

Sub-conclusion: part 2

1. MR measurements can reveal the defects or long-time fluctuations of DW order parameter. These defects lead to the increase of longitudinal MR at field $B \sim B_{MB}$. The cleaner sample is, the stronger is this MR increase. Such increase of MR at is very general and may appear in other DW and even in AFM ordered systems: heavy fermion and high-Tc superconducting materials.

2. In quasi-2D layered compounds DW defects may also lead to the phase inversion of MQO of conductivity.

Global conclusion:

If properly analyzed, the simple transport measurements may give valuable information about electronic systems with DW or AFM order

This is especially helpful in the compounds, where ARPES data are not available because of surface quality or low T_C of DW transition.

Thank you for attention !

Conclusions (Part 2)

The magnetoresistance studies in the density-wave state must take into account additional scattering mechanism from non-uniform MB, which is rather general and depends on DW non-uniformities/defects. This mechanism explains the phase inversion of MQO and MR hump observed in organic metal α-(BEDT-TTF)$_2$MHg(SCN)$_4$

<u>Brief description of this scattering mechanism</u>:

Density wave (DW) with imperfect nesting leads to Fermi-surface (FS) reconstruction.
The DW energy gap $\mathbf{\Delta} \ll \mathbf{E_F}$ separates close electron trajectories in momentum space.
Hence, the magnetic-breakdown (MB) field $\mathbf{B_{MB}} \propto \mathbf{\Delta^2/E_F}$ is easily achieved, which leads to the electron jumps between close classical trajectories

In the crossover regime $\mathbf{B \sim B_{MB}}$, weak spatial non-uniformities of $\mathbf{\Delta}$ strongly change the local MB amplitude, producing additional scattering of conducting electrons.
This leads to magnetoresistance (MR) maximum at $\mathbf{B \sim B_{MB}}$ even at $\mathbf{B \| J}$, and sometimes to phase inversion of the Shubnikov-de Haas oscillations, e.g. as in α-(BEDT-TTF)$_2$MHg(SCN)$_4$.
The cleaner sample is, the stronger is this MR increase due to new scattering mechanism.

Thank you for attention !

Magnetoresistance in layered organic metal α-(BEDT-TTF)$_2$MHg(SCN)$_4$, (M=K,Tl,Rb,..)

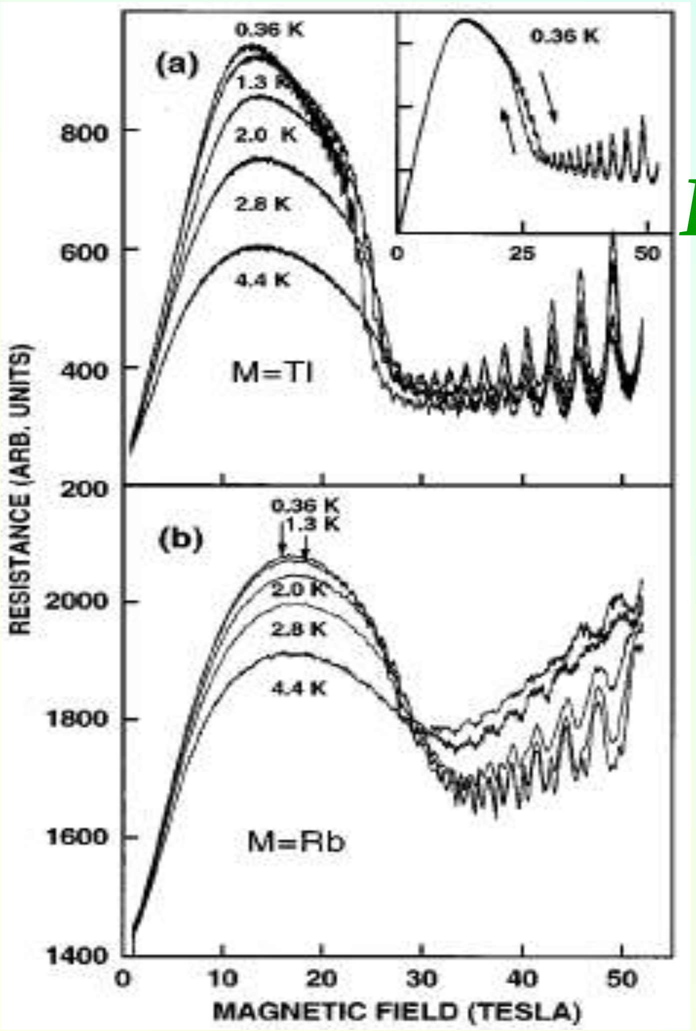

R.H. McKenzie et al., PRB 54, R8289 (1996)

$B \parallel I \parallel z$

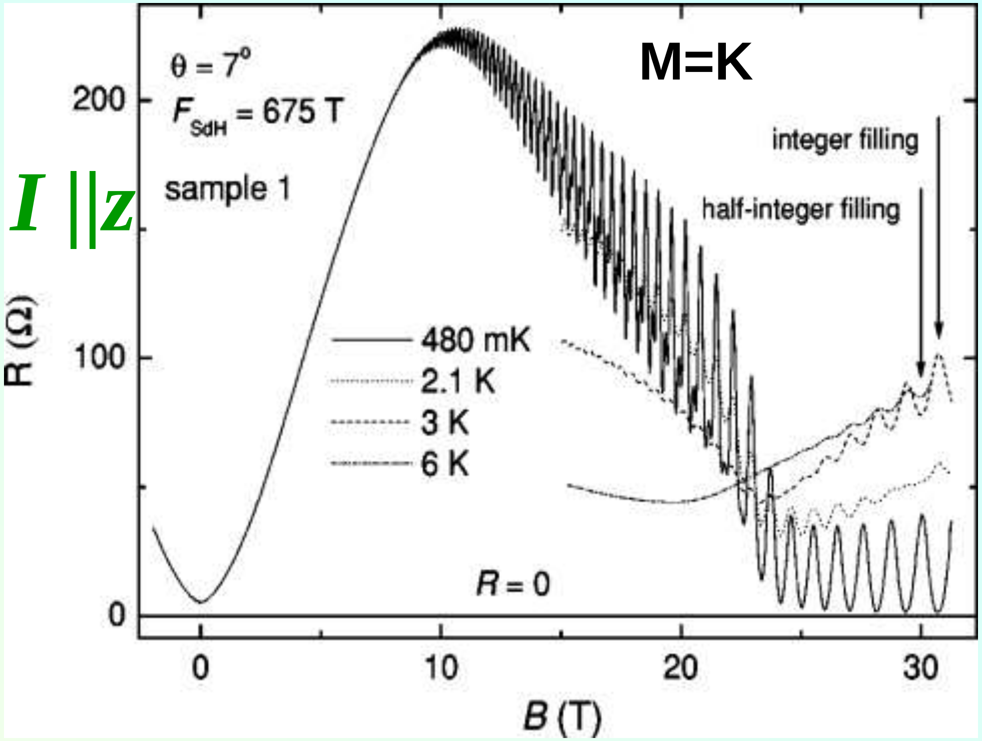

N. Harrison et al., PRB 62, 14 212 (2000)

1. Hump on MR at B~12T
2. Phase inversion of Shubnikov - de Haas oscillations in CDW

Fermi surface reconstruction by CDW

Original in-plane Fermi surface

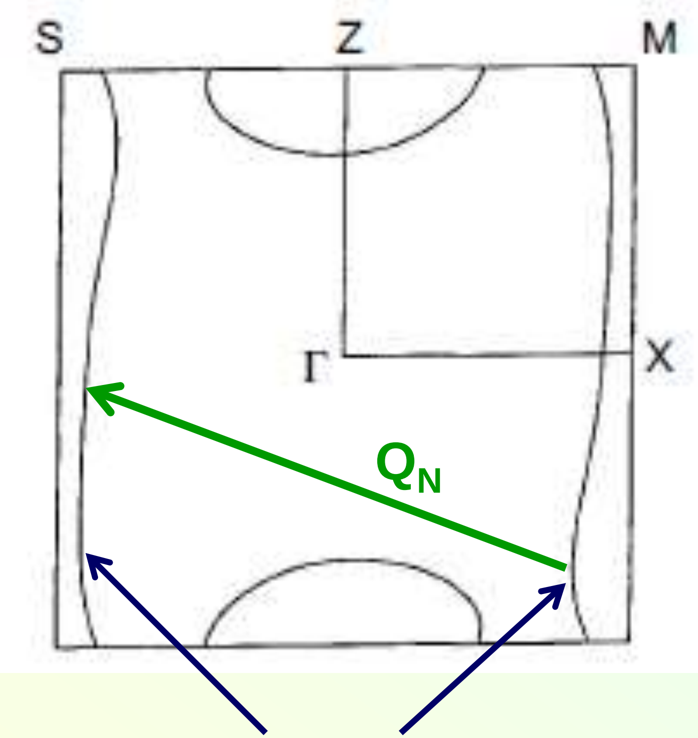

Reconstructed Fermi surface

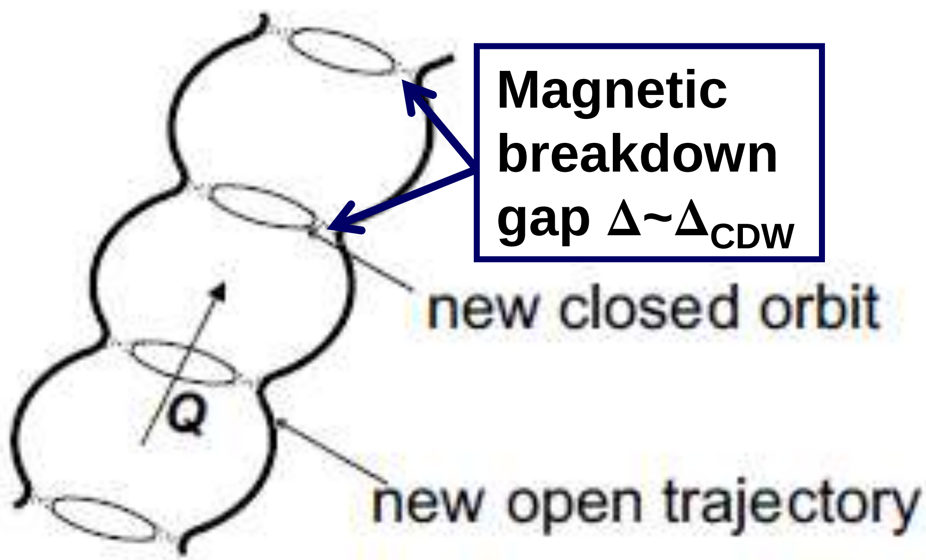

The quasi-1D FS parts possess nesting property with vector Q and become gapped in the CDW state. The CDW creates periodic potential and the new Brillouin zone. The quasi-2D FS pockets then overlap and form reconstructed FS with new quasi-1D sheets and small pockets

For α-(BEDT-TTF)$_2$KHg(SCN)$_4$ this FS reconstruction was first proposed in M.V. Kartsovnik, A.E. Kovalev, N.D. Kushch, J. Phys. I (France) 3, 1187 (1993)

The observed MQO support this FS reconstruction

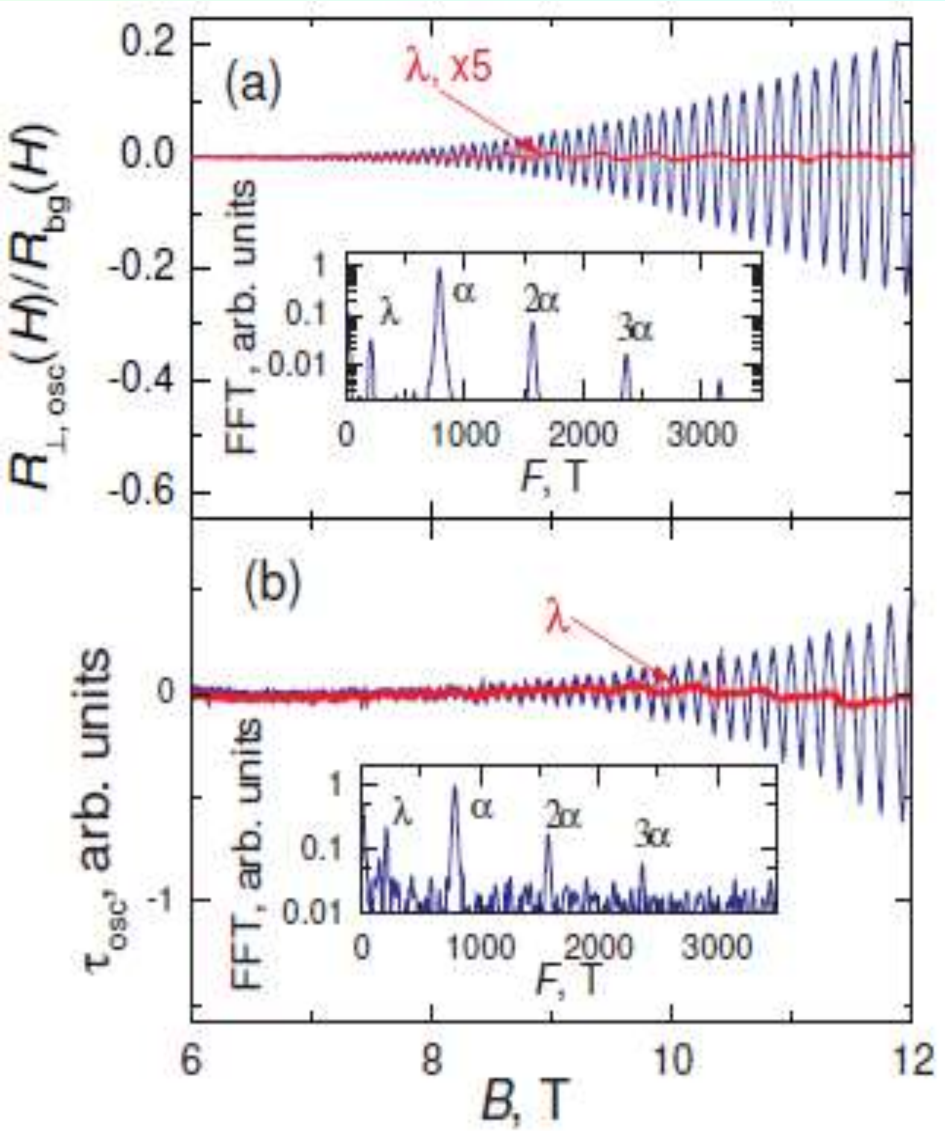

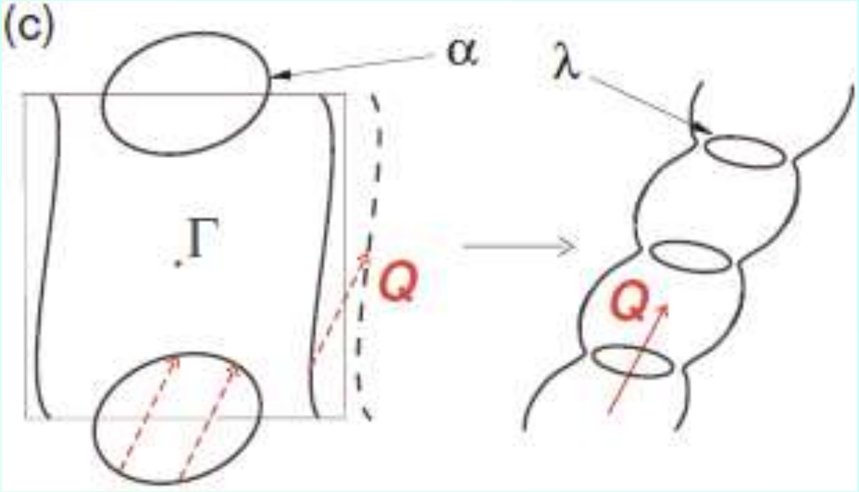

Figure 2. Oscillating components of the magnetoresistance (a) and magnetic torque (b) of the K-salt at $T = 0.45$ K, $\theta = 31.5°$. The red curves are obtained by filtering out the α-oscillations and demonstrate the behavior of the slow oscillations with frequency $F_\lambda = 210$ T. In (a) the λ-oscillations are magnified by a factor of 5, for a better visibility. The insets in (a) and (b) show the corresponding fast Fourier spectra. (c) Schematic 2D view of the Fermi surface reconstruction due to the CDW potential with the wave vector Q. The original Fermi surface (left panel) consists of a pair of open sheets and a cylinder. The CDW, introducing a new periodicity with the wave vector **Q**, opens a gap at the Fermi level in the whole q1D band as well as in the q2D band at the states separated by **Q** (right panel).

FS reconstruction in high-Tc cuprates (just another example)

$Nd_{2-x}Ce_xCuO_4$

(NCCO)

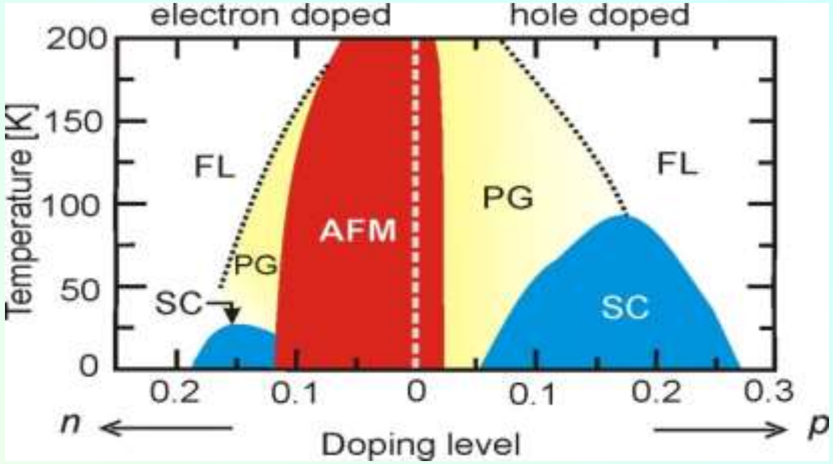

! The Fermi-surface reconstruction is <u>very common</u> and can be easily seen by MQO

Original FS:

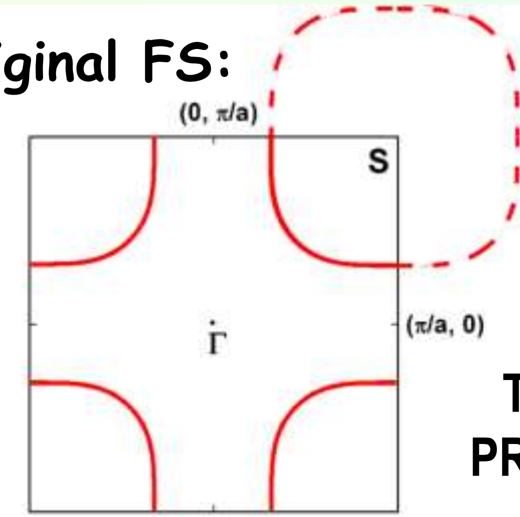

<u>n = 0.17</u>

S_h = 41.5% of S_{BZ}

T. Helm et al., PRL 103, 157002 (2009)

Reconstructed FS:

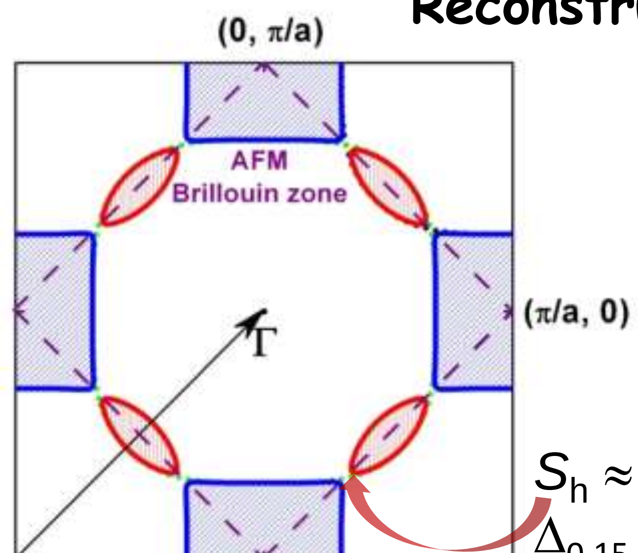

<u>n = 0.15 and 0.16</u>

$S_h \approx$ 1.1% of S_{BZ};
$\Delta_{0.15} \approx$ 64 meV;
$\Delta_{0.16} \approx$ 36 meV

Magnetic breakdown (MB)

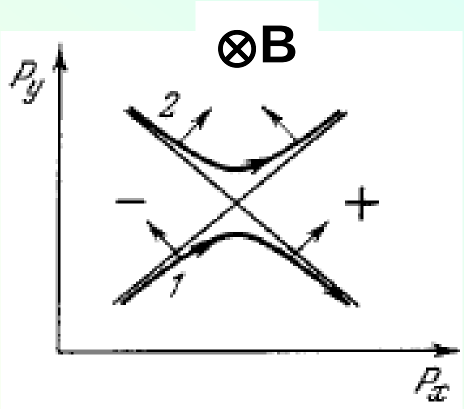

The 2D scattering matrix between states 1 and 2

$$\hat{S} = \begin{pmatrix} \sqrt{1-W}\, e^{i\Lambda}, & -\sqrt{W} \\ \sqrt{W}, & \sqrt{1-W}\, e^{-i\Lambda} \end{pmatrix}$$

where the MB probability $W = \exp\{-H_0/H\}$

the MB field $H_0 \sim \Delta^2/E_F$ is much smaller than gap!

Therefore, the MB is observed very often at available magnetic fields.

Idea: If the CDW gap Δ weakly fluctuates in space (CDW defects), this results in strong fluctuations of the MB probability.

Uniform MB, though strongly scatters conducting electrons, does not lead to the momentum relaxation along field because does not break the spatial uniformity (which gives momentum conservation law).

However, non-uniform MB may give the electron momentum relaxation!

If a local MB defect scatters an electron differently from uniform MB, the electron also changes its momentum along magnetic field => **new scattering mechanism**

Magnetoresistance in layered organic metal α-(BEDT-TTF)$_2$MHg(SCN)$_4$, (M=K,Tl,Rb,..)

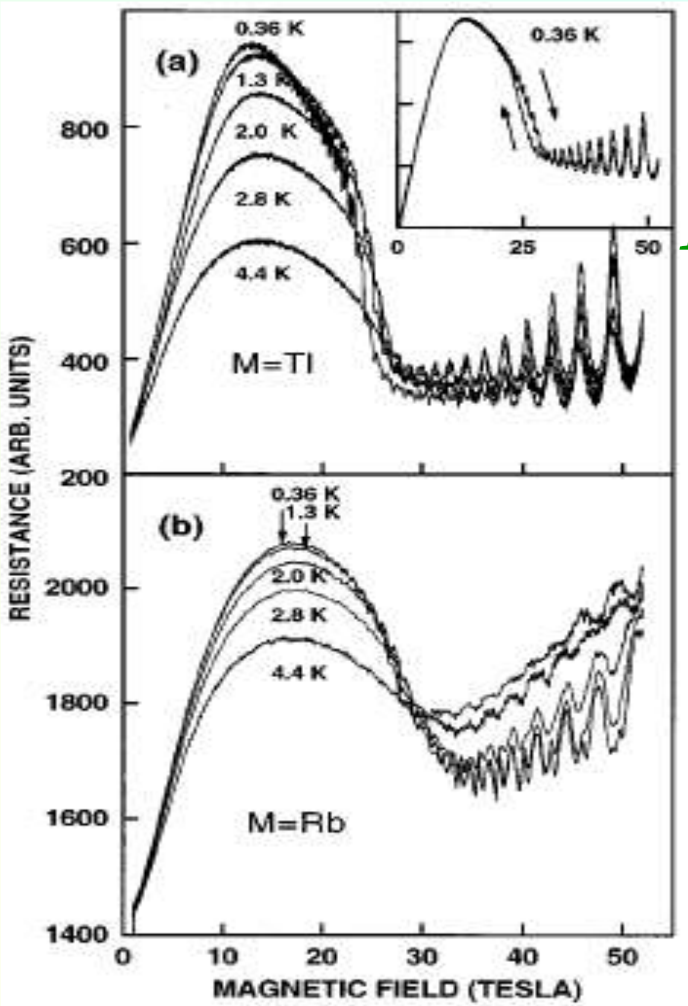

R.H. McKenzie et al., PRB 54, R8289 (1996)

$B \parallel I \parallel z$

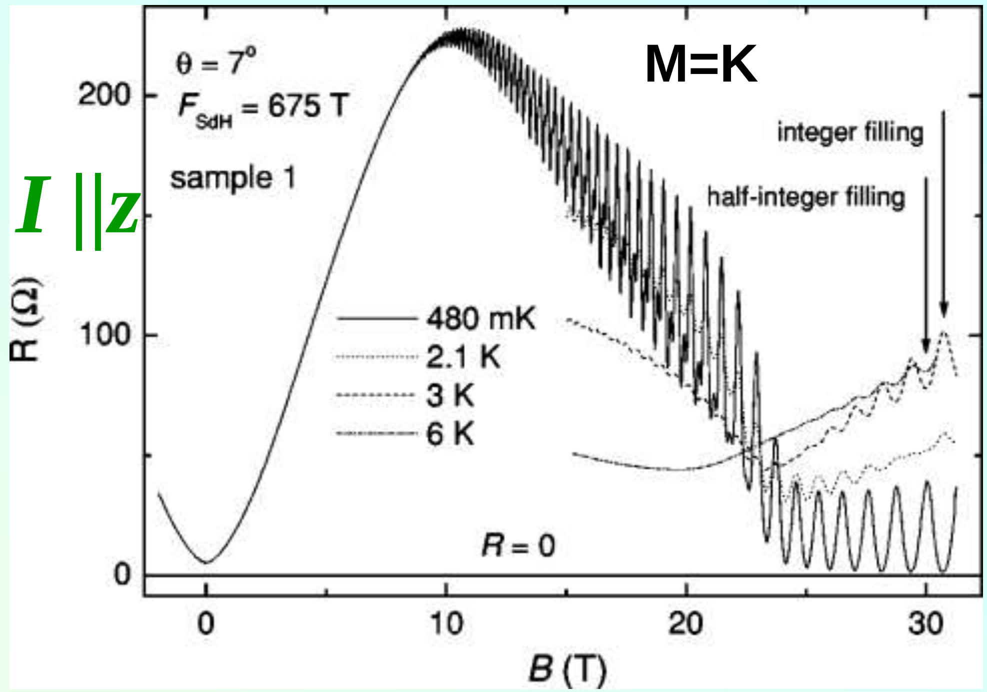

N. Harrison et al., PRB 62, 14 212 (2000)

The observed increase of MR at B~5-20T~H_0 may be due to this new scattering mechanism on MB defects

This mechanism is rather general !

Increased resistivity at MB field H_0 shows the CDW defects

Phase inversion of Shubnikov –de Haas oscillations

Experimental data. The phase inversion is in the dashed region of B-T

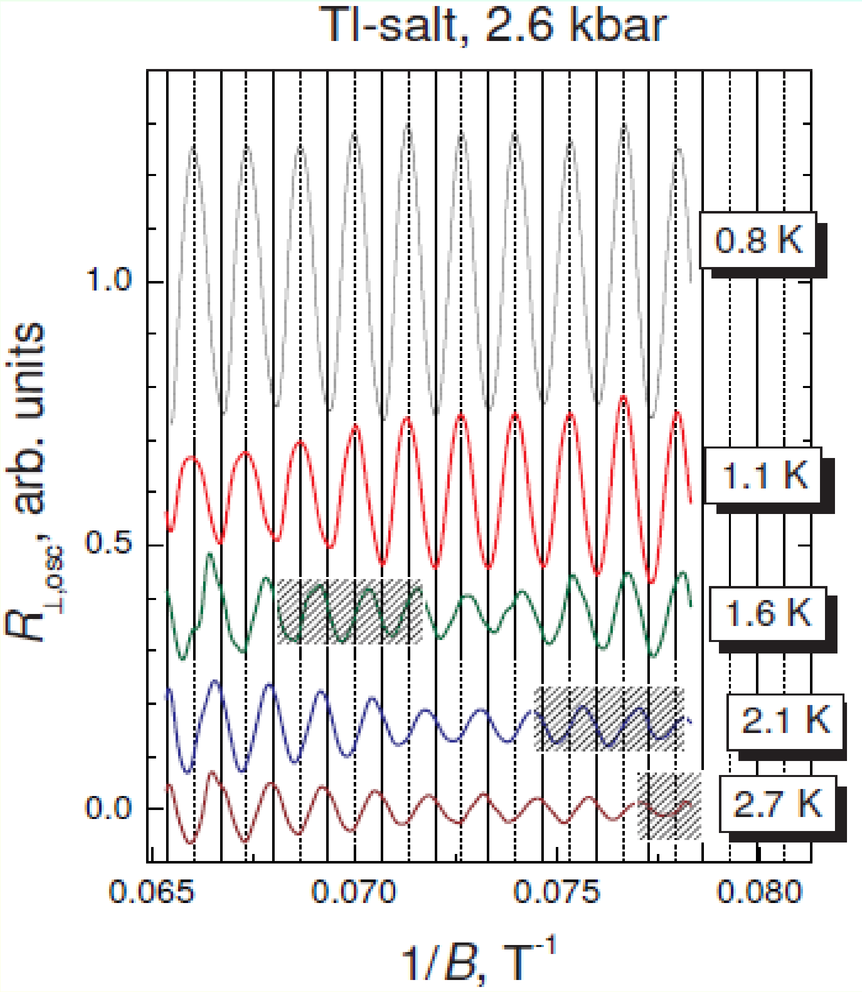

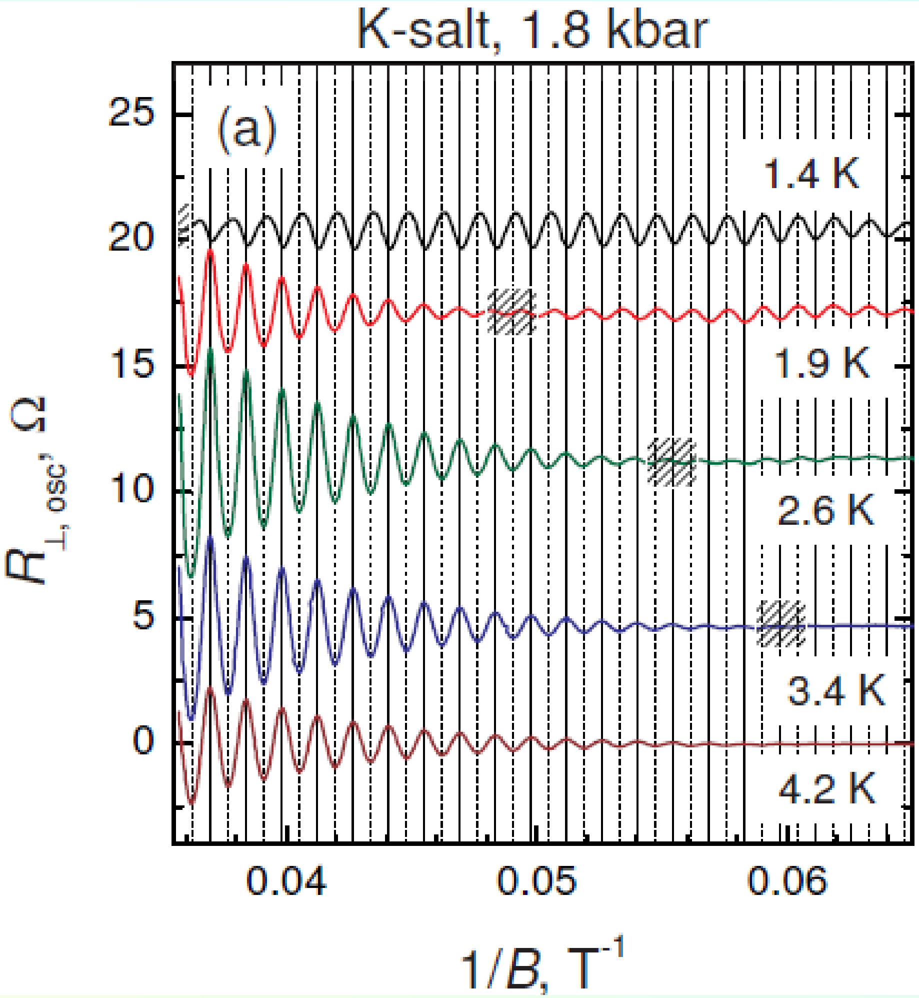

To be published in Low Temp. Phys. [arXiv:1311.5744]

Phase inversion of Shubnikov –de Haas oscillations

The phase inversion comes because the MB scattering is non-diagonal between the FS parts (or, the electron spectrum parts). The defects, increasing the MB amplitude (local reduction of the DW gap), scatter mainly to 2D parts (quantized electron spectrum): $1/\tau_{\mathrm{MB}} \propto \rho_{2D}\left(E_{\mathrm{F}}\right)$

In τ–approximation electron conductivity

$$\sigma_{zz} = 2e^2 \tau_{tot} \sum_{\boldsymbol{k}} v_z^2\left(\boldsymbol{k}\right)\left(-n_F'\left[\varepsilon_{1D}\left(\boldsymbol{k}\right)\right]\right)$$

where the total scattering rate is a sum of MB and impurity contributions: $1/\tau_{tot} = 1/\tau_{\mathrm{MB}} + 1/\tau_i$

When both 1D and 2D parts

$$\sigma_{zz} \propto \frac{\left\langle v_{z1D}^2\right\rangle \rho_{1D}\left(E_{\mathrm{F}}\right) + \left\langle v_{z2D}^2\right\rangle \rho_{2D}\left(E_{\mathrm{F}}\right)}{\rho_{2D}\left(E_{\mathrm{F}}\right)}.$$

$$\left\langle v_{z\,2D}^2\right\rangle(\epsilon) \approx \left\langle v_{z\,1D}^2\right\rangle\left[1 - 2\alpha R_D \cos\left(2\pi\epsilon/\hbar\omega_c\right)\right], \quad \left\langle v_{z\,1D}^2\right\rangle \approx 2t_\perp^2 d^2/\hbar^2$$

The conductivity

$$\boxed{\sigma_{zz} \propto const + \left(\frac{\rho_{1D0}}{\rho_{2D0}} - \alpha\right) 2R_D \cos\left(2\pi F/B\right)}$$

The MQO amplitude changes sign !

Appendices

Phase inversion of Shubnikov –de Haas oscillations

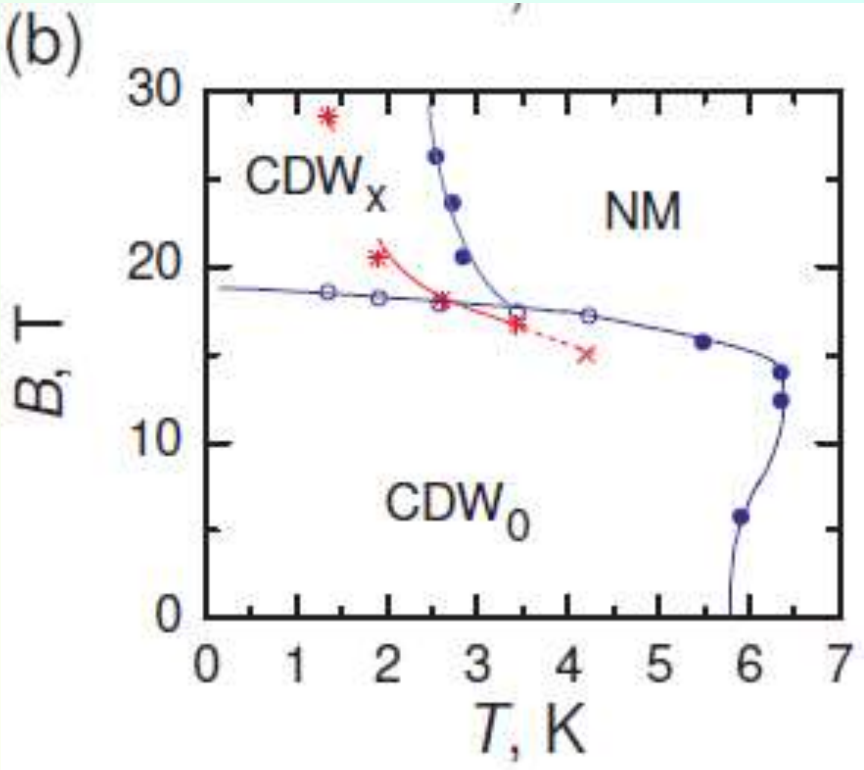

This effect applies only to quasi-2D strongly anisotropic compounds.

Collaboration with M.V. Kartsovnik, V.N. Zverev et al.

To be published in Low Temp. Phys. [arXiv:1311.5744]

Appendix MB

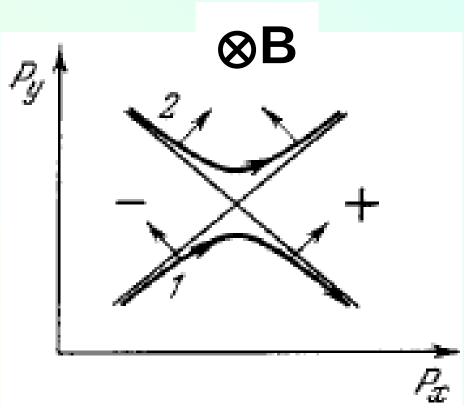

The 2D scattering matrix between the states 1 and 2

$$\hat{S} = \begin{pmatrix} \sqrt{1-W}\,e^{i\Lambda}, & -\sqrt{W} \\ \sqrt{W}, & \sqrt{1-W}\,e^{-i\Lambda} \end{pmatrix}$$

where the MB probability $W = \exp\{-H_0/H\}$

the MB field $H_0 \sim \Delta^2/E_F$ **is much smaller than gap!**

$(B_{MB} \sim \Delta^2 m_c/\hbar e E_F)$

the MB phase $$\Lambda = \frac{\pi}{4} + \frac{H_0}{\pi H} - \frac{H_0}{\pi H}\ln\frac{H_0}{\pi H} + \arg\Gamma\left(i\frac{H_0}{\pi H}\right)$$

Remark: the MB field H_0 can be calculated with coefficient:

If one takes the electron dispersion at the MB point in a general form as

$$\varepsilon_{1,2}(p) = \varepsilon_M + v_M\,\delta p_n + \sqrt{\Delta^2/4 + (v^M_{1,2}\,\delta p_n)^2}\,,$$

$$\varepsilon_M = \tfrac{1}{2}[\varepsilon_1(p_M) + \varepsilon_2(p_m)]\,,\quad \delta p_n = n_M(p - p_M)$$

$$v_M = \tfrac{1}{2}(v^M_{11} + v^M_{22})\,,\quad \Delta = \Delta(p_M) = \varepsilon_1(p_M) - \varepsilon_2(p_M)\,;$$

The MB field H_0 then

$$H_0 = \frac{c\pi\Delta^2}{e\hbar\,|v_x v_{12}\cos\theta|}$$

M.I. Kaganov, A.A. Slutskin, Phys. Reports 98, 189 (1983)

Superconductivity and charge(spin)-density wave

How can these two many-particle phenomena appear together in metals with single conducting band?
or
What is the microscopic structure of this state?

(ungapped electron states on the Fermi level appear when the antinesting term in electron spectrum exceeds SDW or CDW energy gap, and (1) ungapped small Fermi-surface pockets or (2) the soliton band get formed).

How the properties of SC state change on the CDW and SDW backgrounds?

(e.g., the upper critical field diverges at the critical pressure and has unusual T-dependence)

How the spin-structure of SDW (the spin-dependent scattering) affects the SC state?

(it strongly damps the spin-singlet superconductivity.
SC pairing on SDW background is most likely triplet).

Critical magnetic field in the DW-SC coexistence phase

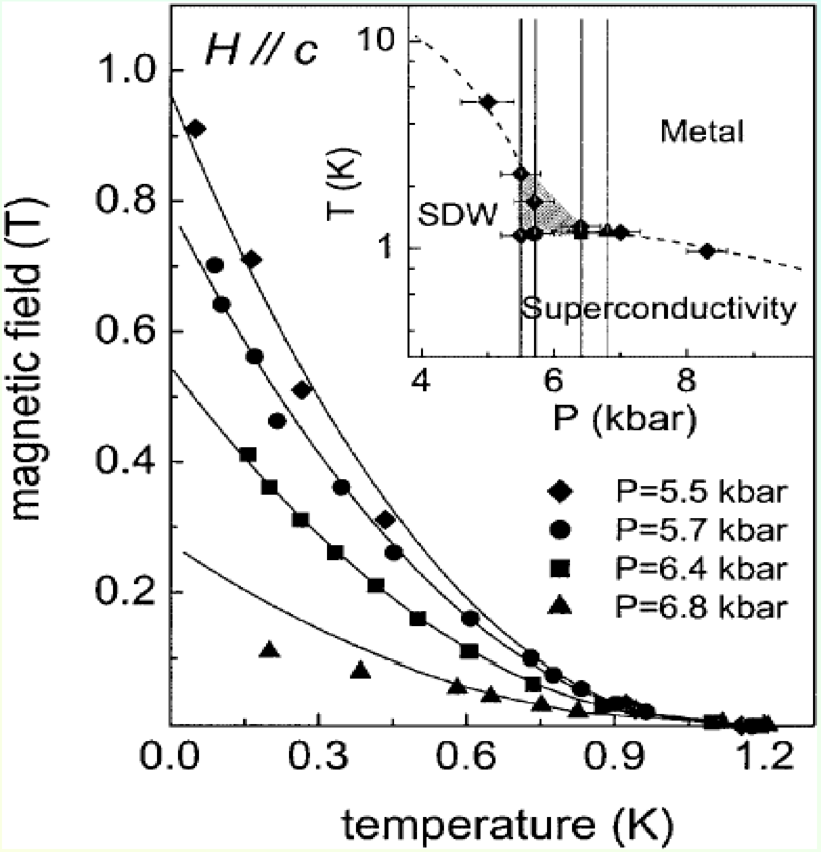

$(TMTSF)_2PF_6$: J. Lee, P. M. Chaikin and M. J. Naughton, PRL 88, 207002 (2002)

CDW + superconductivity:

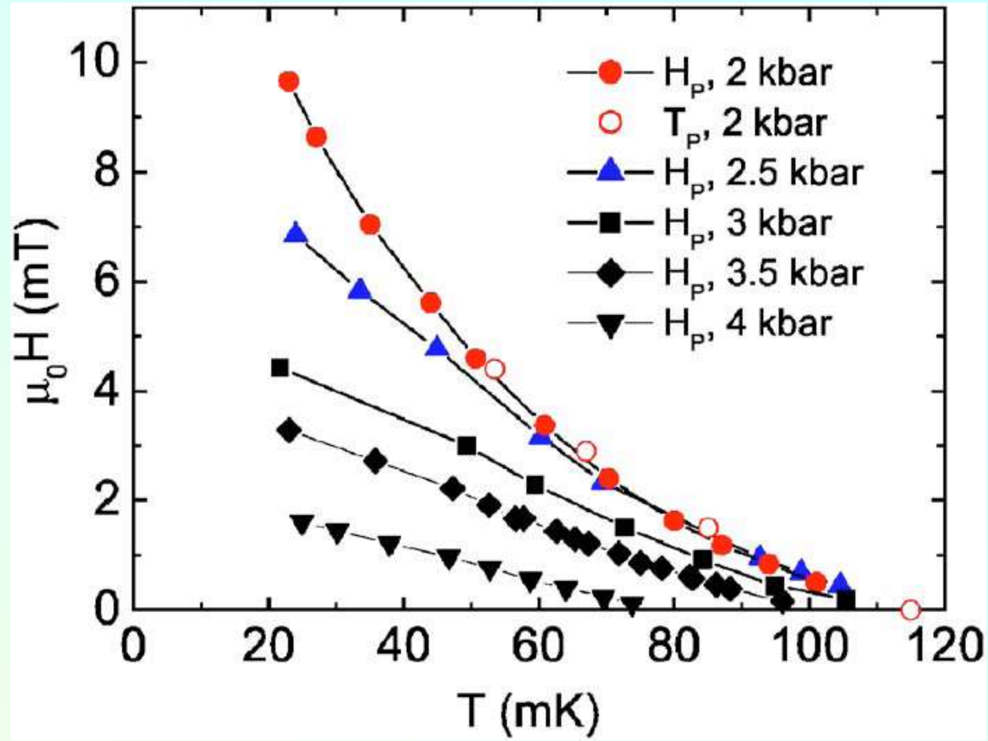

α-$(BEDT\text{-}TTF)_2KHg(SCN)_4$: D. Andres et al., Phys. Rev. B 72, 174513 (2005)

! The critical magnetic field H_{c2} strongly increase and has very unusual temperature and pressure dependence.

Other DW microscopic properties that can be determined from electronic transport experiments

Non-uniformities of the DW order parameter:

1. **Regular defects of DW order (fluctuations, soliton walls, nonuniform CDW – analog FFLO, etc.)**
2. **Irregular defects (e.g., impurities) .**

How these defects reveal in electronic transport ?